The Astrophysical Journal Supplement Series, 192:2 (17pp), 2011 January doi:10.1088/0067-0049/192/1/2

VERY WIDE BINARIES AND OTHER COMOVING STELLAR COMPANIONS: A BAYESIAN ANALYSIS OF THE *HIPPARCOS* CATALOGUE

Ed J. Shaya and Rob P. Olling
Department of Astronomy, University of Maryland at College Park, College Park, MD 20742, USA; eshaya@umd.edu
Received 2010 June 30; accepted 2010 October 28; published 2010 December 13

ABSTRACT

We develop Bayesian statistical methods for discovering and assigning probabilities to non-random (e.g., physical) stellar companions. These companions are either presently bound or were previously bound. The probabilities depend on similarities in corrected proper motion parallel and perpendicular to the brighter component's motion, parallax, and the local phase-space density of field stars. Control experiments are conducted to understand the behavior of false positives. The technique is applied to the *Hipparcos* Catalogue within 100 pc. This is the first all-sky survey to locate escaped companions still drifting along with each other. In the <100 pc distance range, ∼220 high probability companions with separations between 0.01 and 1 pc are found. The first evidence for a population (∼300) of companions separated by 1–8 pc is found. We find these previously unnoticed naked-eye companions (both with $V < 6$th mag): Capella & 50 Per, δ Vel & HIP 43797, Alioth (ϵ UMa), Megrez (δ UMa) & Alcor, γ & τ Cen, ϕ Eri & η Hor, 62 & 63 Cnc, γ & τ Per, ζ & δ Hya, β^{01}, β^{02} & β^{03} Tuc, N Vel & HIP 47479, HIP 98174 & HIP 97646, and s Eri & HIP 14913. High probability fainter companions (>6th mag) of primaries with $V < 4$ are found for: Fomalhaut (α PsA), γ UMa, α Lib, Alvahet (ι Cephi), δ Ara, β Ser, ι Peg, β Pic, κ Phe, and γ Tuc.

Key words: binaries: visual – catalogs – dark matter – proper motions – stars: statistics

Online-only material: color figures, machine readable tables

1. INTRODUCTION

The observed binarity and multiplicity rates of stars are significant clues to star formation processes and galactic dynamics. For example, the mass–ratio distribution among pre-main-sequence binaries[1] indicates that fragmentation rather than common accretion is the dominant formation process (Goodwin et al. 2007). Very wide binaries present a special opportunity because their separations are larger than the size of typical prestellar cores and thus are important for understanding the arrangement of separate stellar disks in low-densities star formation sites (Parker et al. 2009).

After formation, the evolution of binaries is determined by dynamical processes. In high to moderate density environments, most pairs with separations of a few hundred to a few thousand AU are broken up within a few million years (Parker et al. 2009). Outside of these high-density regions, Galactic tides and weak interactions with passing stars peel off stars with separations of a few times 10,000 AU on a timescale of about 10 Gyr (Heggie 1975; Weinberg et al. 1987).

Until quite recently, stars were commonly assumed to quickly leave the scene once they become unbound. However, recent simulations find that escaping stars drift apart with relative velocity $\lesssim 1$ km s^{-1} and remain within a few 100 pc of the primary for billions of years (Jiang & Tremaine 2010). In these simulations, the large-scale potential is dominated by Galactic tides, while local perturbations to the large-scale potential are dominated by stars. Their model does not include molecular clouds, spiral arms, or dark-matter subhalos. The simulations indicate that the binarity rate decreases with separation out until several tidal radii, at which point the rate actually increases and peaks at 100–200 pc. In addition, since the Galactic gravity field dominates the trajectories of escaped stars, they travel along with their ex-primaries, trailing or leading at roughly constant Galactic radii (like a tidal stream, but of only two or three stars).

On the other hand, if, locally, there are many dark matter subhalos, companions would be more quickly torn away and evidence of previous binaries would be lost. Thus, observational determination of the frequency and ages of escaped companions in similar orbits should tell us much about the small-scale structure of the Galactic gravity field, the Oort A- and B-constants, and place stringent constraints on dark matter subhalos.

Existing double star catalogs, such as the Washington Double Star Catalog (WDS; Mason et al. 2001), are mostly populated with systems selected using fairly simple criteria such as proximity in the plane of the sky or common proper motions (CPMs) of high proper-motion stars. Very often, pairs await confirmation of orbital motions before being accepted as a physical pair which, obviously, selects against wide binaries. In a work based on double stars extracted from a large number of catalogs, one of us found that the *apparent* binarity rate changes dramatically both with distance from the Sun, and with apparent magnitude (Olling 2005). In that work many catalogs[2] were combined, and about 90% of HIP stars within 10 pc were found to be either part of a multiple system and/or an exoplanet host. In contrast, only ∼14% of HIP stars are listed as multiple. Furthermore, only ∼2% of HIP stars have other HIP stars as possible companions. Indeed, it appears that the completeness

[1] In this paper, we loosely use the term "binary" to indicate any system that contains more than one star, unless otherwise stated.

[2] The catalogs used were: the *Hipparcos* Catalogue (HIP); Tycho-2 Catalogue (TY2; Høg et al. 2000); *Tycho* Double Star Catalogue (Fabricius et al. 2002); Geneva–Copenhagen Solar Neighborhood Radial Velocity Survey (Nordström et al. 2004); 9th Catalog of Spectroscopic Binaries (Pourbaix et al. 2004; see also http://sb9.astro.ulb.ac.be); 4th Catalog of Interferometric Measurements of Binary Stars (http://ad.usno.navy.mil/wds/int4.html); WDS (Mason et al. 2001; see also http://ad.usno.navy.mil/wds); and Extra-Solar Planets (extracted on 2006 September 11 from http://vo.obspm.fr/exoplanets/encyclo/catalog-main.php). In addition, the updated parallax information from the new Reduction of the *Hipparcos* Catalogue (HIP2; van Leeuwen 2007) is used rather than the values listed in HIP.

of catalogs of field binaries are very seriously affected by selection effects (Hogeveen 1990; Olling 2005; Kouwenhoven 2006; Eggleton & Tokovinin 2008; Kouwenhoven et al. 2009). This is especially true for wide binaries for which confusion due to field stars is severe.

1.1. Why Very Wide Binaries?

Parker et al. (2009) indicate that "hard binaries" with semi-major axis (a) $\lesssim$ 50 AU are almost never affected by dynamical processes in either the field or inside clusters, while "intermediate binaries" (50 AU $\lesssim a \lesssim$ 1000 AU) can be highly affected by dynamical processes, especially if they are formed in dense star clusters. Unevolved "wide binaries" with $a > 1000$ AU can only have formed in low-density star-forming regions with densities less than a few stars per pc^3, the so-called isolated star formation mode (Goodwin 2010). However, of order 15% of G-type dwarfs are found in wide binary systems, with $a \geqslant 10^4$ AU, which even exceeds the size of isolated star formation regions. It is thought that systems of this size can only form during the dissolution phase of low-density clusters (Kouwenhoven et al. 2010).

From a Galactic dynamics perspective, one can expect binary stars with separation up to about the tidal or Jacobi radius, (r_J), while their relative velocities should be about the Jacobi velocity (v_J):

$$r_J = \left(\frac{G\,(M_1 + M_2)}{4\,\Omega\,A}\right)^{1/3} \sim 1.7\,\mathrm{pc}\ , \tag{1}$$

$$v_J \approx 0.05\left(\frac{M_1 + M_2}{2}\right)^{1/3}\ \mathrm{km\,s^{-1}}\ , \tag{2}$$

(Jiang & Tremaine 2010), where G, is the gravitational constant, Ω the angular velocity of the Galaxy at the solar circle, A is Oort's A constant, and M_1 and M_2 are the masses of the components. The value of 1.7 pc is valid for the canonical values for the Galactic constants and individual masses of 1 $M_\odot$. Note that the tidal radius depends weakly, only as the cube root, of total mass. Thus, if it is the case that systems that become unbound remain "close companions" for a very long time, then the region where bound or almost bound systems can be found would extend much farther than has been previously suggested (0.1–0.2 pc; e.g., Heggie 1975; Bahcall & Soneira 1981; Retterer & King 1982; Weinberg et al. 1987; Quinn et al. 2009). This all suggests that separations from 10,000 AU to several parsecs is in need of much further study.

1.2. Some Previous Searches for Very Wide Binaries

The search for companions of high proper-motion pairs in astrometric catalogs is ongoing; e.g., Levine (2005) use the USNO-B1 catalog (Monet et al. 2003), Gould & Kollmeier (2004) use the USNO-B1 and 2MASS (Skrutski et al. 2006), Makarov et al. (2008) use the NOMAD[3] catalog, while Lépine & Shara (2005) and Raghavan (2009) use their own surveys. However, the best astrometric catalogs, HIP, TY2, UCAC2, and now UCAC3 (Zacharias et al. 2010), have somewhat escaped the attention of searches for CPM pairs. We note that Caballero (2009, 2010) has embarked on a program to identify very wide binary systems. His earlier work concentrates on *common* proper-motion systems with separations over 16.′65 in the WDS, while the latter work focuses on the α Lib + KU Lib system with a separation of 2.°6 (1.05 pc). In these works, the focus has been on *common* proper motions. However, to search for the widest bound systems and for recently escaped companions, one must look at separations >1 pc, which corresponds to several degrees of separations for stars within 100 pc. But, projection effects cause companions with similar space velocities to have dissimilar proper motion and radial velocities, hence at very wide separations, *common* proper-motion studies will miss true companions and may even lead to misidentifications. In Section 3.2, we describe how to take these geometric effects into account.

Finding companions of nearby stars by rigorous statistical analyses is a fast way to discover additional nearby stars. It may also be a means of discovering more nearby brown dwarfs and white dwarfs, provided many faint candidate stars are included, as in the larger Tycho-2 (TY2) or UCAC3 catalogs. Finally, the discovery of a substantial number of late-type stars that are paired to higher mass stars can help significantly in establishing the metallicity and temperature scales for these low-mass systems (presumably, both components have the same (Fe/H)).

Therefore, it would be fruitful to attempt to construct a statistically robust catalog of astrometric companions (both bound systems and escaped binary components) with well defined selection criteria by data mining modern astrometric catalogs. The astrometric catalogs such as HIP, TY2, UCAC3, and NOMAD provide order of magnitude better proper motions than previous catalogs (but see the cautionary notes by Makarov et al. 2008 on possible systematic errors for faint NOMAD sources). In this paper, a methodology based on Bayesian statistics is discussed and applied to the stars in just the HIP that are within 100 pc. In a future work, we will present results of applying these techniques to stars in the TY2 that may be companions to stars in HIP.

Throughout this paper, we use "d" for distance (in pc), "r" for three-dimensional radial separation, "π" for parallax, "μ" for proper motion, "θ" for angular separation, and "a" for semi-major axis, unless otherwise stated. The subscripts and superscripts "p," "c," and "f" are used to refer to properties of primaries, companion candidates, and stars in "the field," respectively.

2. MULTIPLICITY: RECENT DEVELOPMENTS

In their study, (Duquennoy & Mayor 1991, hereafter DM91) use their radial velocity (RV) data in combination with existing astrometric binaries to determine the distribution of periods of main-sequence (MS) G stars within 22 pc. They find that the parent distribution function (PDF) of periods is approximately Gaussian in the logarithm of the period,

$$\mathrm{PDF}(\mathcal{P}) \propto e^{-\frac{1}{2}\left(\frac{\log_{10}\mathcal{P} - 4.8}{2.3}\right)^2}\ , \tag{3}$$

where $\mathcal{P}$ is the period in days. The peak is at $\mathcal{P} = 173$ years ($\sim$35 AU), while the 1σ boundaries are 316 days ($\sim$1 AU) and 34,000 years ($\sim$1212 AU). From their data, DM91 estimate a binary fraction of $\sim$67%. DM91 also find that their observations are consistent with the assumption that secondaries are drawn randomly from the initial mass function (IMF) below the primary; therefore, companions are usually considerably fainter than the primary. There is debate in the literature over the exact shape of the PDF: DM91's Gaussian shape was first proposed by Kuiper (1942) versus Öpik classical power-law

[3] The NOMAD catalog is a compiled catalog containing positions, proper motions, some optical colors, *and* NIR colors from 2MASS, if available. The astrometric data listed come from the HIP, TY2, UCAC2 (Zacharias et al. 2004), and USNO-B catalogs.

Table 1
Parameters for Probability Estimator

Distance (pc)	$\Delta\mu_{\rm lim}$ (mas yr^{-1})	$\Delta\mu_{\rm inner}$ (mas yr^{-1})	$\Delta\mu_{\rm outer}$ (mas yr^{-1})	$\Delta d_{\rm max}$ (pc)	$\theta_{\rm inner}$ (deg)	$\theta_{\rm outer}$ (deg)	μ_0 (mas yr^{-1})	α_0 ...	$\Delta\mu_1$ (mas yr^{-1})	α_1 ...	$N_f^{\rm max}$ ...
0–25	35	45	100	20	0.01	20	10.0	0.97	7.13	0.97	None
25–50	25	35	75	15	0.01	10	3.44	0.93	3.39	0.78	12
50–100	10	20	50	20	0.005	5	2.09	1.06	2.28	1.15	10

distribution (Öpik 1924). Because the integral of the Öpik-power-law distribution diverges, it *must* break down. This is indeed observed at small and large separation (e.g., Goldberg et al. 2003; Chanamé & Gould 2004; Lépine & Bongiorno 2007, and references therein).

Raghavan (2009), in his dissertation, presents an impressive body of work on a sample of stars that significantly extends the DM91 sample. He scrutinized 454 Sun-like stars within 25 pc by pulling together up-to-date RV surveys and the best *Hipparcos* astrometry, while he also performed a large survey with the CHARA interferometer for close-in binaries. Following in the footsteps of recent wide-binary searches, he "blinked" between early- and late-epoch sky-survey images, out to radii of about $10'$, or 10 kAU. He concludes that (55 ± 3)% of stellar systems are single stars. For the 25 pc sample, we search for companions with separations up to 120 times larger than those blinked by Raghavan (2009).

3. METHODOLOGY

Although astronomers have been searching for and finding physically associated pairs of stars since the time of Galileo, there have not been thorough studies to explicitly assign probabilities of association. In this pilot project, we search for common proper-motion stellar multiples out to very large separations, as far as is practical, and set probabilities for these to be more than merely coincidental. We do *not* limit ourselves necessarily to high proper-motion pairs as has been done in the past (Gould & Chanamé 2004; Lépine & Bongiorno 2007): although stars with field stellar density exceeding some threshold in a five-dimensional box given by distance, plane of the sky positions and proper motions are dropped. A region about the provisional primary star that is the same extent in sky coordinates as the field selection region but much smaller in proper motion is used to provide high quality candidate companions. Where the field density is small, any star appearing in this small region has high probability of being physically associated. As the field density increases, false positive detections grow and eventually swamp true companions. In the range between these, it should be possible, using control experiments, to at least provide upper limits to the number of real companions along with a set of candidates each with moderately low probabilities. These candidates can be followed up with RV measurements to further assess their true nature.

The results of the *Hipparcos* space-based mission provide high precision proper motions and parallaxes using only its 3.5 year baseline. For many cases, though, the best proper motions are obtained from catalogs that combine data from several astrometric catalogs, spread over up to 100 years. In our current study, we use the proper motions from TY2 when available, and from HIP2 otherwise. Although the HIP2 errors are often smaller than the TY2 errors, it is important to use proper motions over a longer baseline than that of HIP2 to ensure that the barycentric motion is used. A tight secondary at a few AU could induce proper motions of the primary at several times the HIP2 error. In the DM91 distribution, since about one-half of all binaries have periods <173 yr ($a \lesssim 35$ AU) then, within 50 pc, the orbital motions are several to tens of mas yr^{-1}, significantly larger than the proper-motion errors. Thus, the longer time baseline of TY2 makes its proper motions less susceptible than HIP2 to orbital motions induced by small separation companions. One magnitude below their respective completeness limit, HIP2 has errors in proper motion of $\epsilon_\mu \sim 0.8$ mas yr^{-1} at $V \sim 8.5$, while TY2 has $\epsilon_\mu \sim 3.5$ mas yr^{-1} at $V = 11.5$.

As each cataloged star is considered as a primary, all stars within a radius of $\theta_{\rm outer}$ and more than $\theta_{\rm inner}$ (Table 1), within a distance range $\mid d - d_p \mid < \Delta d_{\rm max}$, and with $\Delta\mu = \mid \vec{\mu}_c - \vec{\mu}_p \mid < \Delta\mu_{\rm outer}$ are selected. Of those stars, the number outside of $\Delta\mu_{\rm inner}$ define the *local* star-density ρ_f. Those stars within a specific proper-motion difference, $\Delta\mu_{\rm lim}$, become candidates for companions. This value is chosen by examining the simulation and finding a value that lets in roughly 90% of the simulated binaries. One can change this parameter to either somewhat reduce the false positive rate or to allow in lower probability candidate companions.

3.1. Bayesian Statistics

Our procedure for determining the probability that two stars are physical companions relies on observed proper-motion differences, $\Delta\vec{\mu} = \vec{\mu}_p - \vec{\mu}_c$, angular separation θ and positional differences of stars within a chosen range of brightness. We are not necessarily looking for bound systems; rather we seek systems that are unlikely to be the results of random distributions. RV differences are not a metric in these statistics because presently the fraction of stars with known radial velocities is small except for very nearby bright stars and because a star's RV can be perturbed by a close companion. It is quite typical for spectroscopic binaries to have offsets in measured radial velocities by 20 km s^{-1} from the true barycentric velocities. With time the barycentric velocities can be determined by averaging, but often this is not yet adequately done. However, for cases in which radial velocities are known and where the barycentric motion is determined, radial velocities can be used to assess the statistical goodness of the technique of probability assignment.

All stars within a specified range in the observables are considered to be candidate companions or simply "candidates," provided that they are fainter than the provisional primary star. This jargon is chosen for simplicity of bookkeeping, even though, of course, the brightest star in a system is not always the most massive component.

Bayesian statistics can provide an estimate of the probability of association for each candidate. Given multiple observables, O_i, that each provide some discrimination on the two possibilities, either the star is a companion (c) or it is a field star (ie, not c or $\neg c$), the standard Bayesian formula in this case is

$$P(c \mid O_1; O_2; ...; O_i) = \frac{\prod_i P(O_i \mid c)P(c)}{\prod_i P(O_i \mid c)P(c) + \prod_i P(O_i \mid \neg c)P(\neg c)}, \quad (4)$$

where the numerator has the product of available probabilities for each observable having its observed value assuming that the candidate is a companion, $P(O_i|c)$. The numerator also includes a prior probability term, $P(c)$, in which knowledge of the companion probability of the ensemble of candidates or additional knowledge of the companions can be introduced. If no prior knowledge is available, then this term can be set to $\frac{1}{2}$, and at least one will have a rank ordering in the probabilities of the candidates. The denominator has a repeat of the numerator, plus a similar product of probabilities, except this time the assumption is that the candidate is not a companion.

For this work, the discriminating observables are radial separations r from parallax and proper-motion differences $\Delta\mu$, so the above formula for the posterior probability of being a companion is

$$P(c \mid r;\Delta\mu) = \frac{P(\Delta\mu \mid c)P(r \mid c)P(c)}{P(\Delta\mu \mid c)P(r \mid c)P(c)+(1-P(r \mid c))(1-P(r \mid c))(1-P(c))}. \quad (5)$$

With the prior P(c) set to 0.5 this provides probabilities with a starting assumption that each candidate is just as likely to be a field star as a companion. One can improve on this by providing the probability of being a companion based on statistics of the field stars that are nearby in angle, proper motion, and distance separation Δd:

$$P(c) = \frac{(1-P(\Delta d \mid f))(1-P(\Delta\mu,\theta \mid f))P(p)}{(1-P(\Delta d \mid f))(1-P(\Delta\mu,\theta \mid f))P(p)+P(\Delta d \mid f)P(\Delta\mu,\theta \mid f)(1-P(p))}. \quad (6)$$

Here, $P(\Delta d \mid f)$ is the probability that one or more field stars fall with radial distance less than the candidate's distance from the primary. Therefore, $(1 - P(\Delta d \mid f))$ is the probability that no field stars randomly fall in this range. The term $P(\Delta\mu, \theta \mid f)$ is the probability that one or more field stars happens to have proper motion and angular separation more similar to the primary than the candidate.

The term $P(p)$ is the probability that the provisional primary, selected in the manner in which it has, is a primary, i.e., it has at least one wide companion in the radial region that we are exploring. It is perhaps somewhat dismaying at first that $P(p)$ is needed to derive individual probabilities since normally the individual probabilities would be needed to derive it. However, as we show, it is possible to conduct control experiments, using the actual catalog data, to constrain $P(p)$.

3.1.1. $P(\Delta\mu \mid companion)$ and $P(r \mid companion)$

To calculate the probability that a binary star would have a given proper-motion difference, one could calculate the intrinsic probability density function of velocities for random orbits from Kepler's Laws and take into consideration distances, errors in distances, and errors in proper-motion observations. The probability of having some specified observed proper-motion difference $\Delta\mu$ assuming it is a companion is given by the complementary cumulative distribution function (CCDF) which is the integral of the PDF over proper-motion differences greater than the observed value:

$$P(\Delta\mu \mid c) = \iint_{\mu>|\Delta\mu|} PDF(\Delta\vec{\mu})dA_{\vec{\mu}}. \quad (7)$$

However, it is more straightforward to create a simulation of the star catalog (described in Section 3.3), add simulated binary orbits, add observational errors and then form the histogram of the distribution of proper motions. Per Equation (7), the cumulative distribution is reversed and this provides estimates of the probability of a companion to have the observed proper-motion value. These probabilities are fit sufficiently well by the following form for the components parallel and perpendicular to the motion of the primary:

$$P(\mu_\perp \mid c) = \exp[-(\mu_\perp/\mu_0)^{\alpha_0}], \quad (8)$$

$$P(\Delta\mu_\parallel \mid c) = \exp[-(\Delta\mu_\parallel/\Delta\mu_1)^{\alpha_1}]. \quad (9)$$

The probability that a companion would have both components greater than the observed ones is

$$P(\Delta\mu \mid c) = 1-(1-P(\mu_\perp \mid c))(1-P(\Delta\mu_\parallel \mid c)). \quad (10)$$

The parallel and perpendicular coordinates are used here because our first-order error analysis indicates that most geometric effects will be parallel to the motion of the primary (see Section 3.2 and Equation (29) below).

For the probability based on observed three-dimensional radial separation, we calculate the period $\mathcal{P}$ using $(\mathcal{M}_p + \mathcal{M}_c)\mathcal{P}^2 = r^3$ and apply it to the CCDF of the DM91 distribution modified to allow for individual errors in parallax that reflect into errors in r and period of the orbit. The CCDF of this log-normal distribution is given by the complementary error function:

$$P(r \mid c) = \mathrm{erfc}\left(\frac{\log(\mathcal{P})-4.8}{\sqrt{2}\sqrt{2.3^2+\epsilon^2_{log\mathcal{P}}}}\right). \quad (11)$$

Of course, for radial separations of several parsecs where the system is no longer bound the DM91 distribution looses meaning, but it continues to be useful in providing a steeply descending function.

The error in r is given by

$$\epsilon_r^2 = \Big[\left(\left(\epsilon_{\pi_p}x_p^2\right)^2+\left(\epsilon_{\pi_c}x_c^2\right)^2\right)(x_p-x_c)^2 \quad (12)$$

$$+\left(\left(\epsilon_{\pi_p}y_p^2\right)^2+\left(\epsilon_{\pi_c}y_c^2\right)^2\right)(y_p-y_c)^2 \quad (13)$$

$$+\left(\left(\epsilon_{\pi_p}z_p^2\right)^2+\left(\epsilon_{\pi_c}z_c^2\right)^2\right)(z_p-z_c)^2\Big]/r^2. \quad (14)$$

But, we need the error in the log of the period due to uncertainty in distance,

$$\epsilon_{\mathcal{P}} = \frac{3r^2}{2\mathcal{M}P}\epsilon_r = \frac{3\mathcal{P}}{2r}\epsilon_r \quad (15)$$

$$\epsilon_{\log\mathcal{P}} = \frac{\epsilon_{\mathcal{P}}}{\mathcal{P}\ln(10)} = \frac{3\epsilon_r}{2\ln(10)r}. \quad (16)$$

3.1.2. $P(\Delta\mu, \theta \mid field)$ and $P(\Delta d \mid field)$

We seek the probability that one or more field stars would have a proper motion as close or closer to the primary as the candidate given the local density if stars per unit spatial and proper-motion area. The number density is given by

$$\rho_f = \frac{N_f}{\pi^2\left(\Delta\mu^2_{\mathrm{outer}}-\Delta\mu^2_{\mathrm{inner}}\right)\left(\theta^2_{\mathrm{outer}}-\theta^2_{\mathrm{inner}}\right)}. \quad (17)$$

The formula for the probability of one or more stars, chosen from a homogeneous distribution with this density, falling at separation less than θ and proper-motion difference less than $\Delta\mu$ is

$$P(\Delta\mu, \theta \mid \text{field}) = 1 - e^{-\pi^2 \rho_f \theta^2 \Delta\mu^2}. \quad (18)$$

Even though this formula is formally for a constant density distribution it works well for a density changing linearly in the coordinates. However, near the peak of the density distribution with proper motion along a line of site, the curvature in the density profile can cause substantial error in the local density and it is best to simply avoid this calculation near the peak. Since the peak is where the density becomes very high and probabilities are low, this region needs to be avoided anyway. Therefore, we only consider primaries with a field density below a given threshold (Table 1).

The probability that one or more field stars would happen to have an observed distance that is less than the Δd observed for a candidate star is given by similar formulae,

$$\lambda_f = \frac{N_f}{2\Delta d_{\max}} \quad (19)$$

$$P(\Delta d \mid \text{field}) = 1 - e^{-\lambda_f \Delta d}. \quad (20)$$

3.2. Geometrically Induced Proper-motion Differences

With increasing stellar separation there is a growth in the proper-motion difference caused by various projection effects, even if the two stars have the same space motion. However, in most cases some compensation can be made for this. We can first look mathematically at the gradient of $\vec{\mu}$ due to spatial separations at constant space velocity. To search for very wide binaries, we start by presuming space velocities are essentially the same for the system's stars. For a binary with a solar mass primary separated by more than 0.01 pc, the orbital velocities are $< 0.78\,\mathrm{km\,s^{-1}}$. Beyond 25 pc, this corresponds to $\lesssim$6.6 mas yr^{-1} in proper-motion differences. In Galactic coordinates (ℓ, b), the vector of proper motion is composed of the two projections of the three-dimensional velocity onto the unit vectors in the longitude and latitude directions divided by the distance d to the star:

$$\hat{\boldsymbol{\ell}} = \frac{\hat{z} \times \vec{\boldsymbol{d}}}{\|\hat{z} \times \vec{\boldsymbol{d}}\|} = (-\sin\ell,\ \cos\ell,\ 0), \quad (21)$$

$$\hat{\boldsymbol{b}} = \frac{\vec{\boldsymbol{d}} \times \hat{\boldsymbol{\ell}}}{\|\vec{\boldsymbol{d}} \times \hat{\boldsymbol{\ell}}\|} = (-\sin b \cos\ell,\ -\sin b \sin\ell,\ \cos b), \quad (22)$$

$$\vec{\boldsymbol{\mu}} = (\mu_\ell, \mu_b) = \left(\frac{\vec{\boldsymbol{v}} \cdot \hat{\boldsymbol{\ell}}}{d},\ \frac{\vec{\boldsymbol{v}} \cdot \hat{\boldsymbol{b}}}{d}\right), \quad (23)$$

$$\mu_\ell = (-v_x \sin\ell + v_y \cos\ell)/d \quad (24)$$

$$\mu_b = ((-v_x \cos\ell - v_y \sin\ell)\sin b + v_z \cos b)/d \quad (25)$$

$$v_r = (+v_x \cos\ell + v_y \sin\ell)\cos b + v_z \sin b\,, \quad (26)$$

where $\hat{\mathbf{z}}$ is the unit vector to the north Galactic pole. If distances are in pc and proper motions are in as yr^{-1}, then the radial velocities are in AU yr^{-1} (1 AU yr^{-1} $\simeq$ 4.74 km s^{-1}). The velocity $\vec{\mathbf{v}}$ is relative to the sun so it is formally $\vec{\boldsymbol{v}}_* - \vec{\boldsymbol{v}}_\odot$, where $\vec{\boldsymbol{v}}_\odot$ is the velocity of the sun in the local standard of rest (LSR).

The derivatives of the direction vectors,

$$\frac{\partial\hat{\boldsymbol{\ell}}}{\partial\ell} = (-\cos l,\ -\sin l, 0), \qquad \frac{\partial\hat{\boldsymbol{\ell}}}{\partial b} = (0, 0, 0), \quad (27)$$

$$\frac{\partial\hat{\boldsymbol{b}}}{\partial l} = -\hat{\boldsymbol{\ell}}\sin b, \qquad \frac{\partial\hat{\boldsymbol{b}}}{\partial b} = -\hat{\boldsymbol{d}}, \quad (28)$$

can be used to derive the gradients in spherical coordinates to get a first-order assessment of the geometric induced variations on the difference in proper motion between two stars moving at the same space velocity:

$$\Delta\vec{\boldsymbol{\mu}} = -\vec{\boldsymbol{\mu}}\frac{\Delta d}{d} + \left(\mu_b \sin b - \frac{v_r}{d}\cos b,\ -\mu_\ell \sin b\right)\Delta\ell + \left(0, -\frac{v_r}{d}\right)\Delta b\,, \quad (29)$$

where $\Delta\ell$ and Δb are the difference in longitude and latitude, in radians. Similarly, we can look at the first derivatives of the RV which, if known for both components, can be taken into account when assessing whether the pair is really comoving:

$$\Delta v_r = d\,(\mu_\ell \cos b \Delta\ell + \mu_b \Delta b)\,. \quad (30)$$

As an example, let us examine a case where $b = 45^\circ$, $\mu_\ell = \mu_b = 0.2$ as yr^{-1}, the RV is -20 km s^{-1}, the primary's distance is 20 pc, the companion is 1 pc farther away than the primary, and they are separated by 1 degree per coordinate ($\Delta\ell = \Delta b = 0.0175$, separation $\sim\frac{1}{2}$ pc). We then have

$$\begin{aligned}\Delta\mu_\ell &= -0.2 \cdot 1/20 + \frac{\sqrt{2}}{2}(0.2 + 20/(4.74 \cdot 20)) \cdot 0.0175 \\ &= -0.02\,\text{as yr}^{-1} = -20\,\text{mas yr}^{-1}\end{aligned}$$

$$\begin{aligned}\Delta\mu_b &= -0.2 \cdot 1/20 + \left(-\frac{\sqrt{2}}{2} \cdot 0.2 + 20/(4.74 \cdot 20)\right) \cdot 0.0175 \\ &= -9\,\text{mas yr}^{-1}\end{aligned}$$

$$\Delta v_r = 4.74 \cdot 20 \cdot 0.2\left(\frac{\sqrt{2}}{2} + 1\right) \cdot 0.0175 = 0.6\,\mathrm{km\,s^{-1}}\,.$$

Note that the changes in proper motions can be quite significant with respect to the measurement errors (typically 1–3 mas yr^{-1} and 1–3 km s^{-1}). This implies that very wide binaries of several degrees in separation are, in general, not found by commonality in proper motions, unless proper geometric corrections have been applied.

Equation (29) implies that when relative distances are unknown, one can still make useful corrections using the proper motions and radial velocities. And, when radial velocities are also unknown one can still make useful corrections, by assuming $v_r = 0$, that become highly accurate for $\Delta\mu_\ell$ near the poles.

Also, one can mitigate somewhat against large uncertainty in the Δd term in Equation (29), by taking note that this term is parallel to a system's overall proper motion. Therefore, one should treat the parallel and perpendicular components of the

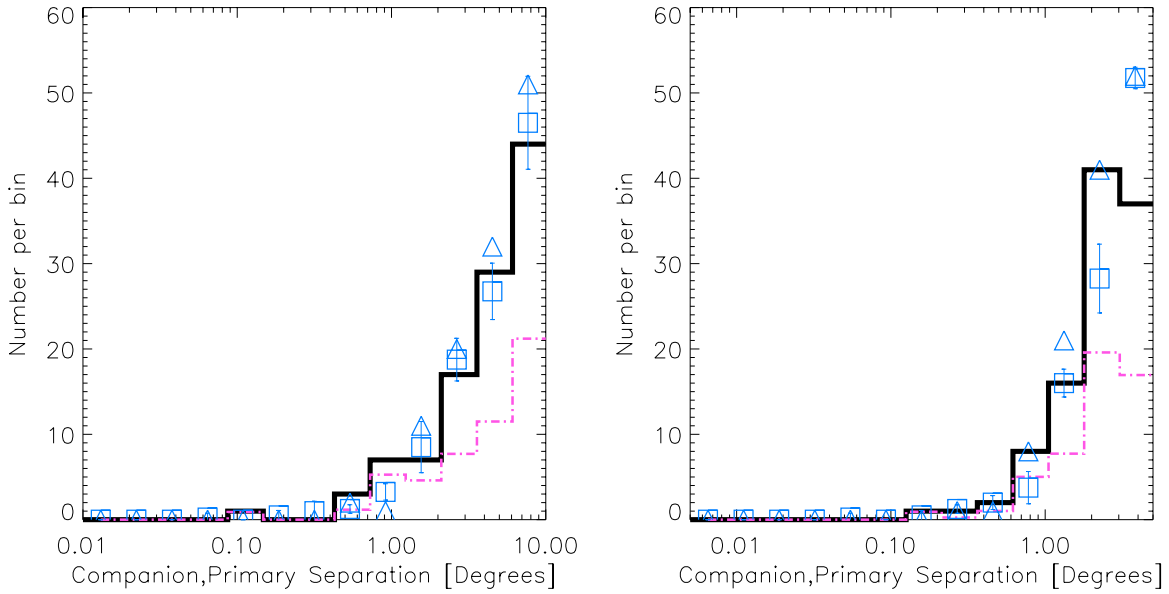

Figure 1. Simulation: number vs. angular separation with no companions—the local neighborhood is simulated but with no binary systems included. The diagrams show numbers of companions per logarithmic separation bin with probability >10%. Since there are no companions here, these are all false positives. The left side shows results for primaries between 25 and 50 pc, and the right side is for 50–100 pc. The solid thick line gives the numbers found in an analysis of the simulation similar to one we do for the *Hipparcos* Catalogue. The control experiment in which $b = -b$ for the primaries is shown as triangles. The average over 4 "rethrow" control experiments is shown as blue squares and the variance is shown in error bars. The purple dash-dotted line is the sum of the probabilities of companions within each separation bin.

(A color version of this figure is available in the online journal.)

proper motion separately to take advantage of the perpendicular component which needs no Δd correction term and hence is less noisy.

The first-order correction, Equations (29), is typically good to $\lesssim$10% for angles $< 5^\circ$and distance differences of <30%, except near $b = \arctan(v_r/d\mu_b)$ where the $\Delta\mu_l$ term goes to zero for changes in angle. To explore out to separations of $\sim 10^\circ$ and reach several pc physical separations, a full (nonlinear) correction for space velocities is made. We calculate the three-dimensional space velocity of each primary from its proper motion and RV (Equations (31)–(33)), if we have it, and, using Equations (24) and (25), calculate the proper motion that this space motion implies, *if it were in the direction of each companion candidate*. If there is no RV for the primary, then the system is assumed to be at rest in the LSR. In those cases, the projection of the the solar motion in the radial direction is subtracted, using (10.0, 5.25, 7.17) km s^{-1} for the solar motion. As described in Section 4.1, for $d < 100$ pc, there are RV measures for most of the primaries.

The conversion to space velocities is the inverse of Equations (24)–(26) and has the solution

$$v_x = v_r \cos b \cos \ell - d\mu_\ell \sin \ell - d\mu_b \sin b \cos \ell \quad (31)$$

$$v_y = v_r \cos b \sin \ell + d\mu_\ell \cos \ell - d\mu_b \sin b \sin \ell \quad (32)$$

$$v_z = v_r \sin b + d\mu_b \cos b. \quad (33)$$

To avoid excessive error arising from distance uncertainties at distances beyond 25 pc, we assume the companion is at the distance of the primary.

3.3. Simulation

A program for creating simulations of the solar neighborhood distribution of stars with binary systems was written to test the methodology, search for optimal parameters, and to understand the origin and behavior of false positives. The simulations cover a large range of parameters to understand the reliability and broadness of applicability of the methodology. The simulations also are used as a quick way to derive the shape of the cumulative distribution functions for the observables in an ensemble of random binary systems.

In the simulations, stars are set down with a distribution of positions and velocities that statistically imitate the HIP2 after observational errors are included. Observational errors representative of moderately faint stars in TY2 are used: $\epsilon_\mu = 1.5$ mas yr^{-1}, $\epsilon_\ell = \epsilon_b = 1$ mas. For parallax errors of the simulated stars, we use $\epsilon_\pi = 1$ mas to represent the HIP2 data. Masses are distributed with the power law $N \sim M^{-2.3}$ from 0.8 to 15 $M_\odot$ and luminosities follow a mass–luminosity relation, $L \sim M^{-3.5}$. An arbitrary fraction of the stars are given companions. The companions do not themselves host companions, e.g., no hierarchical systems are created. The orbital elements: eccentricity, inclination, longitude of the ascending node, longitude of the periapsis, and epoch are random uniform distributions. The distribution of periods is chosen to be log-normal without a long period cutoff.

We first present the relatively small false positive rate for a simulation in which no binary stars were generated. In Figure 1, the numbers of companions with probabilities >0.1 versus angular separation are shown (black thick solid line), where the associated primaries are in the 25–50 pc (left) and 50–100 pc (right) distance ranges. The "false positive" rate is kept low by using a low value for the prior $P(p)$, namely 0.20 for 25–50 pc and 0.07 for 50–100 pc. These values for $P(p)$ are chosen because they work reasonably well for all that follows.

Figure 2 shows results of an analysis of a simulation in which the semi-major axes are set by the DM91 distribution of periods but using only periods longer than the peak of the distribution at 173 yr. About 21% of the stars are primaries and 28% are

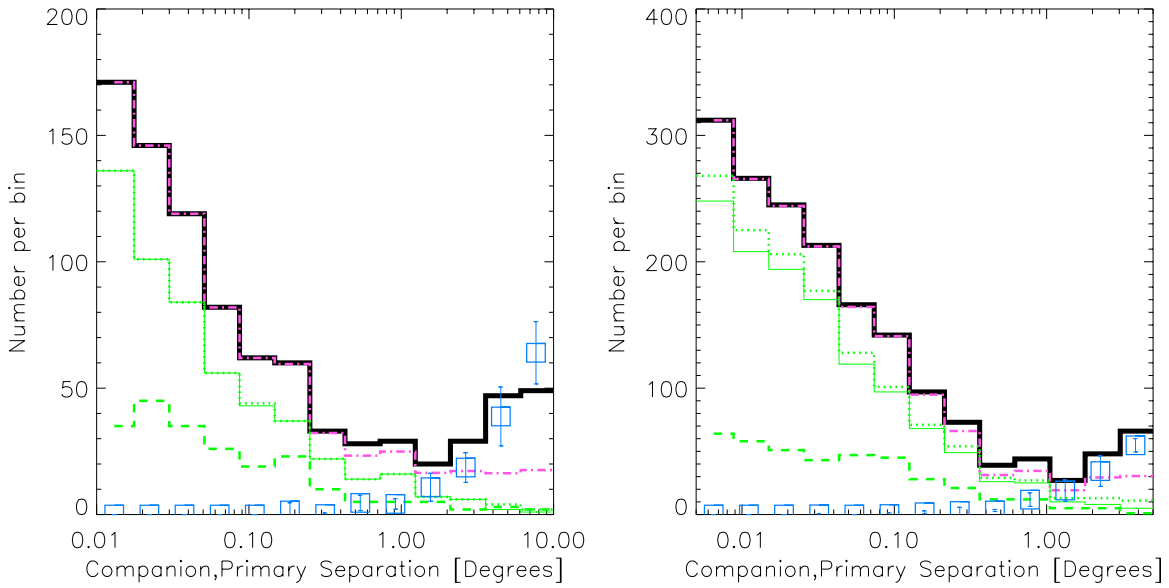

Figure 2. Simulated number vs. angular separation with DM91 binary distribution—results of a simulation with about 50% of the stars being physically related companions that follow the DM91 binary distribution. The left plot is for primaries between 25 and 50 pc, and the right is for 50–100 pc. The green dotted line shows the number of companions per logarithmic separation bin created in the simulation within the distance interval. The black solid line shows the number of companion candidates found with probabilities >10%. The green thin solid line gives the number of these that are correct primary–companion associations and the lower green dashed line gives the number where the primary was missed but two companions are scribed to be a primary–companion pair. The average over four rethrow control experiments plus a reversal of Galactic latitude is shown as blue squares with error bars. The purple dashed-dotted line is the sum of the probabilities of companions within each bin.

(A color version of this figure is available in the online journal.)

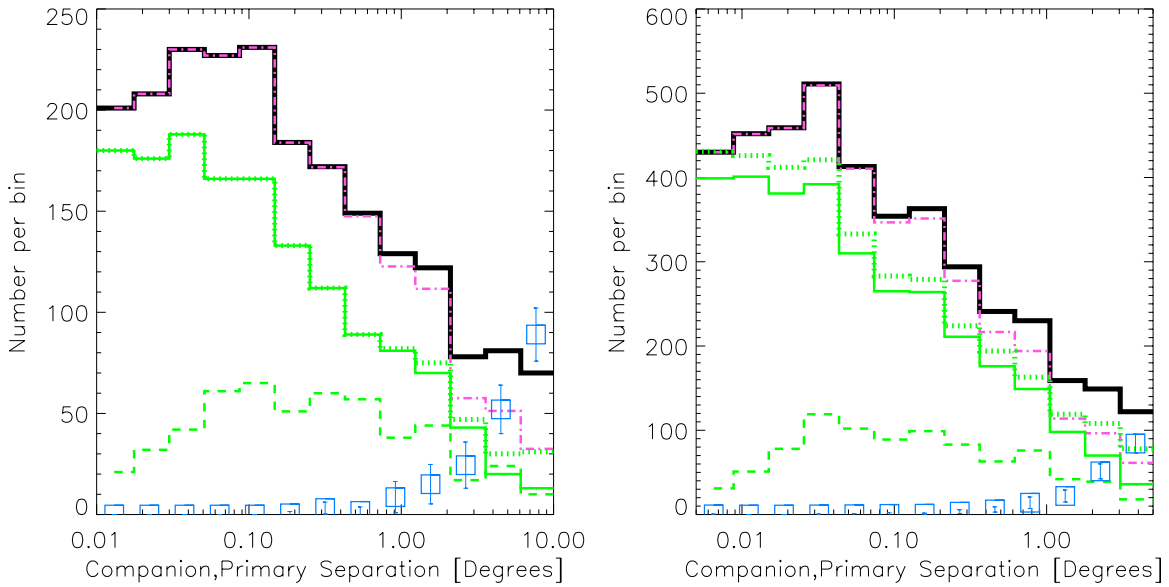

Figure 3. Simulated number vs. angular separation with expanded DM91 binary distribution—same as previous figure, but periods of the bound systems were multiplied by 100 to produce more companions at much larger radii. Now one can compare at very wide separations how many primary–companions are correctly caught (green thin solid line) compared to how many are in the simulation (green dotted line).

(A color version of this figure is available in the online journal.)

companions. These rates are much higher than the observed one, considering that the mass function only goes down to 0.8 $M_{\odot}$, but it provides many companions and much confusion to better test the procedure. The primaries have one, two, three, or four companions with frequency of roughly 67.8%, 27.4%, 4.5%, and 0.2%, respectively. The green dotted line shows the number of companions created per separation bin. The solid thick line shows the number of companions found with probabilities >10%. The green thin solid line gives the number of correct primary–companion associations found. The lower green dashed line gives the number of companions ascribed to be primary–companion pairs, but neither was an input primary, i.e., it gives the number of secondary–tertiaries pairs, etc., found. The procedure recovers better than 90% of the multiple systems for separations out to 2° for 25–50 pc and 1° for 50–100 pc or about a parsec.

In Figure 3, the period distribution for the simulation is multiplied by 100 to shift the distribution to larger semi-major axes. Now, one can see that there is still reasonable recovery (>20%) of companions even at separations of 10° for 25–50 pc

Table 2
Attrition of Primary Stars

Distance	$V < 10$	Has Field	$N_f < N_{f,\max}$	Has Cs	No. of Cs $P > 0.1$	No. of Ps $P_p > 0.1$	$N_c - N_c^{\rm ctrl}$	$(N_c - N_c^{\rm ctrl})(< 1$ pc)	$\sum P$	$\sum P_{<1\,\rm pc}$
0–25	1041	786	786	369	144	111	84	34	85.7	26.9
25–50	4152	2916	2889	1119	316	265	194	89	198.7	72.5
50–100	14064	9018	8861	2090	504	464	258	99	301.3	106.5
Total	19257	12720	12536	3578	964	840	536	222	585.7	205.9

Notes. Column 1: distance interval of the row; Column 2: number of stars brighter than $V = 10$; Column (3): number left after removing stars with no field stars or candidate companions; Column 4: number left after removing those with too high field phase-space density; Column 5: number left after removing those with no candidates; Column 6: number of candidates with $P > 0.1$; Column 7: number of primaries with at least 1 candidate with $P > 0.1$; Column 8: number of candidates − number of candidates in control experiments with $P > 0.1$; Column 9: Same as Col. 8, but separations < 1 pc only; Column 10: $\sum P$ for candidates with $P > 0.1$; Column 11: $\sum P$ for candidates with $P > 0.1$ and separated by less than 1 pc.

region and 5° for 50–100 pc. For 0–25 pc, we get good fractional recovery until 20°.

The resulting distributions of observables for this simulation are used to set the coefficients presented in Table 1. These coefficients do not depend on the fraction of stars that hold binaries, nor do they depend strongly on the shape of the separation distribution. They do depend fairly strongly on the assumed observational errors which essentially determine the widths of the cumulative distributions. However, as the width of the distributions change, the value of $P(p)$ needs to adjust in a direction to keep the sum of the probabilities constant near the values indicated by the control experiments (next section). The net result is that the assigned probabilities change rather slowly with the observational errors assumed.

3.4. Control Experiments

We implement two kinds of control experiments that use the observed data directly rather than the simulation to assess the rate of false positives and thereby determine the prior probability $P(p)$. Using the real data for control tests provides greater confidence that minor differences between the simulation and reality do not cause inconsistencies. In the first method, the negative of the Galactic latitude is used for each star while it is considered as a primary. This moves the primary away from its companions and places it in a region with similar stellar density and velocity field. Any stars assigned high probabilities are statistical coincidences or false positives. Although there is asymmetry between the two hemispheres in the observed proper-motion distribution, much of this goes away after transforming to the LSR and the remaining should have a small affect on the numbers of false positives.

In the second method, all candidates are removed from each primary, and then each field star is randomly "rethrown" with new uniform random two-dimensional positions within the separation angle limit, $\theta_{\rm outer}$, and random values of $\Delta\mu$ within a circle in coordinates $(\Delta\mu_\parallel, \mu_\perp)$ whose size is set to maintain the density in phase-space. The field star distances and brightnesses are maintained. When the control experiments are run on a simulation with zero binaries, the two control methods and the direct analysis of the simulation returns approximately the same number of false positives, within each probability bin, as they should. The first method of control experiment, with the reverse sign of b value of each primary, is shown as blue triangles in Figure 1, where no binary stars are generated in the simulation. The second method, with field star rethrown, is shown as blue squares with error bars at the average and rms deviations of four realizations. For the other figures showing number versus separation, both types of control experiments are averaged together and shown as blue squares.

4. APPLICATION TO THE *HIPPARCOS* CATALOGUE

As a first application of our Bayesian probability estimator, Equations (5) and (6), we examine stars in the HIP2 brighter than 10th mag in V band for possible companion stars brighter than $V = 12$. Provisional primaries are separated into three distance intervals, by parallax distance. There are 1,041 potential primaries ($V < 10$) within 25 pc, 4152 in the 25–50 pc shell, and 14,064 in the 50–100 pc shell. A 15° radius around the Hyades is cut out when working with the 25–50 pc primaries. A 200′ radius around the Pleiades Cluster and also around the Coma Star Cluster are cut out for 50–100 pc primaries. Stars with $\pi < 5$ mas are presumed to be too far away and are also removed. For companions, about 25,000 stars are brighter than $V = 12$ and are within 110 pc.

Candidate companions and field stars are selected if their separation from the primary is $36'' < \theta_{\rm lim} < 20°$ for $d_p < 25$ pc, $36'' < \theta_{\rm lim} < 10°$ for $25 < d_p < 50$ pc, and $18'' < \theta_{\rm lim} < 5°$ for $50\ {\rm pc} < d_p < 100$ pc, (Table 1). Most HIP binaries closer than 36″ and within 50 pc would already be known and their proper-motion differences may be substantially affected by orbital motion, while our methodology is optimized for the case of low orbital speeds. Companions are not constrained to come from the same distance interval as the primary star. Table 2 presents how many potential primaries there were in each distance range and the numbers remaining after dropping ones with no stars nearby, then no candidates, then too high of a field density, and finally presents the number of primaries and candidates with probabilities over 0.1. The total probabilities given for all candidates in the entire separation range and for just those with separations <1 pc.

Table 1 provides the final set of parameters that are used in the analysis of each distance intervals and in creating the tables and figures in this section. In addition to the coefficients for the cumulative distributions in each of the observables and the cutoffs in angle and proper motion for candidates and for field star counts, the table includes the maximum number of field stars accepted. Most field stars along a given direction are concentrated in a small range of proper-motion: consistent with expectation from the Galactic rotation and the projection of the solar motion along the line of sight. If the phase-space of the star is well centered in this "cloud," usually, the probabilities for any companions would naturally be low and the rate of false positives unacceptably high. To avoid this, a star is dropped if the field phase-space density is above the 90th percentile in the

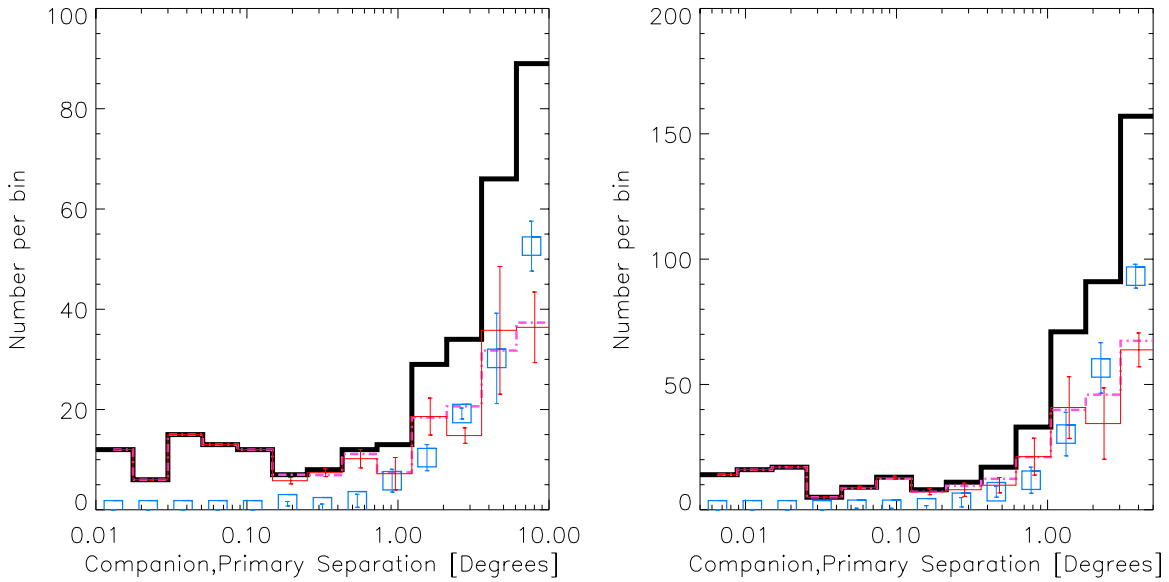

Figure 4. Number vs. angular separation of *Hipparcos* companions—results of the *Hipparcos* Catalogue for primaries between 25 and 50 pc (left) and for 50–100 pc (right). The black thick solid line shows the number of companions found with probabilities >10%. The averages over four rethrow control experiments and one reversal of Galactic latitude are shown as blue squares with error bars. The red thin line with error bars shows the observed minus the averages of the control experiments and therefore provides an estimate of the number of real companions in the *Hipparcos* Catalogue. The purple dash-dotted line is the sum of the companions' probabilities within each bin. Note how different this figure is from the previous figures of simulations.

(A color version of this figure is available in the online journal.)

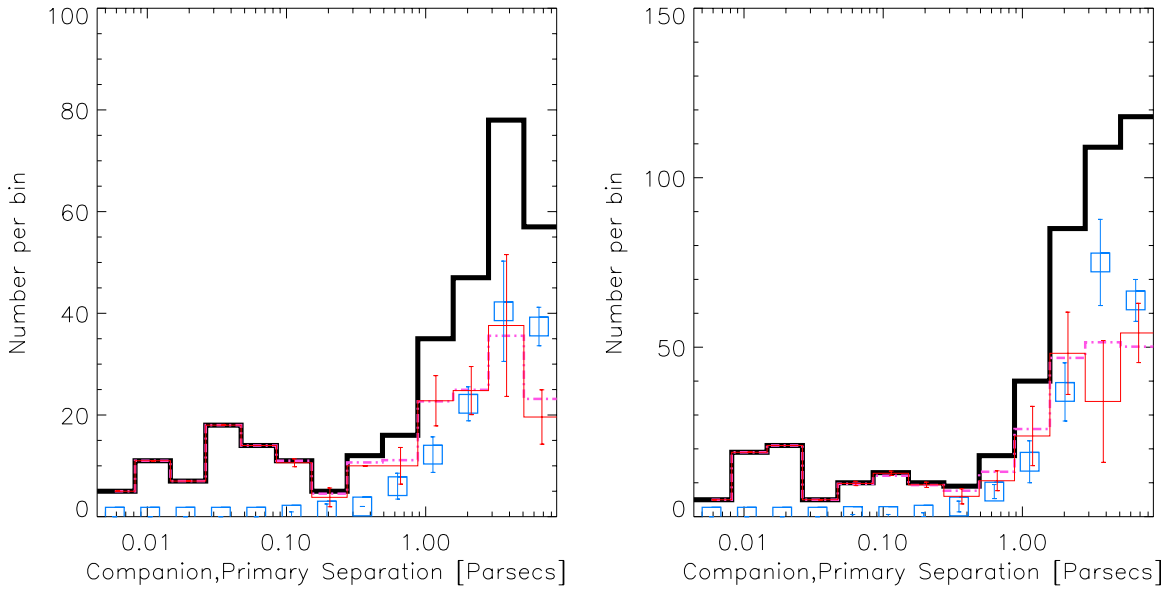

Figure 5. Number vs. physical separation of *Hipparcos* companions—same as in previous figure, but bins are now in logarithmic separation in parsecs based on parallax measurements of primaries.

(A color version of this figure is available in the online journal.)

density distribution. However, in the 0–25 pc region, the number of candidates is always small, so, it is unnecessary to include this criterion there.

Histograms of the separation distributions for the HIP catalog are shown in Figure 4 (in degrees) and Figure 5 (in parsecs). In each diagram, the black thick line is the histogram of companions with $P > 0.1$, the blue square symbols are the averages over five control experiments, and the red lines shows the numbers found minus the numbers in the control experiments, providing an estimate of the range of real physical companions (red error bars). The choice for $P(p)$ is simply the value that brings the sum of the probabilities in each bin into agreement with the number of companions found minus the number in the control experiments. The sum of the probabilities of companions within each separation bin (purple dash-dotted line) has been adjusted by varying $P(p)$, settling at a value of 0.20 for 25–50 pc and 0.07 for 50–100 pc.

The degree of agreement is startling to the authors. Since the actual distribution at these separations is very different from the DM91 distribution used in $P(r|c)$, one might worry that it would not work at all. However, all that is required for this probability is a function that falls off rapidly enough to sufficiently suppress the false positives, and the DM91 law happens to work.

For separations up to $\approx$1 pc the number of false positives found in the control sample is quite small implying that the companions found in the real sample are reliable. The

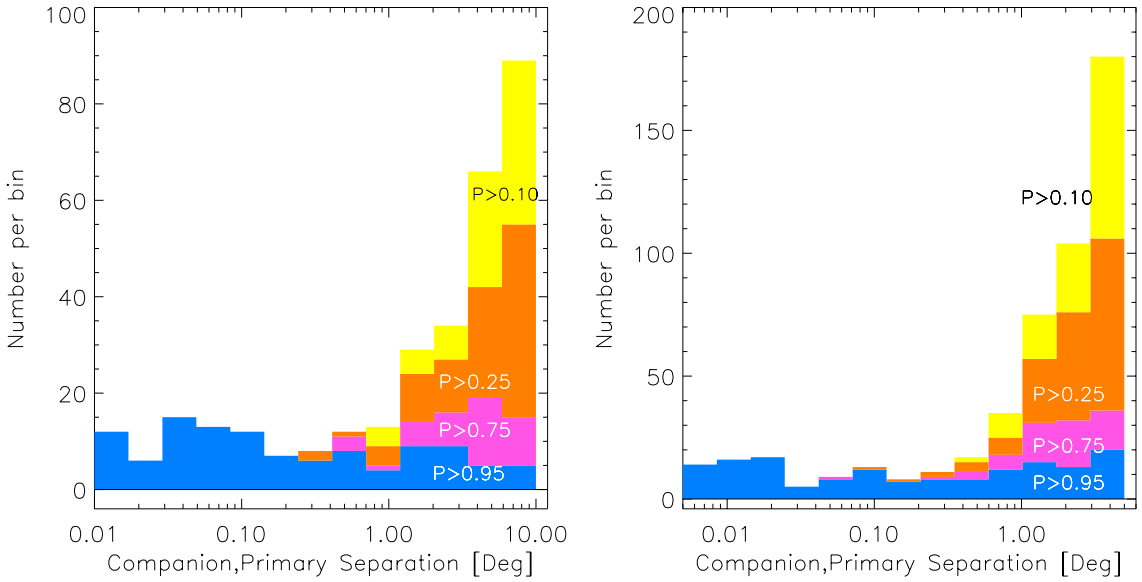

Figure 6. Number and probability vs. angular separation of *Hipparcos* companions—the companion separation histogram showing the contributions from different probability ranges. The contribution from probabilities >0.95 is blue, $0.75 < P < 0.95$ is green, $0.25 < P < 0.75$ is orange, and $0.1 < P < 0.25$ is yellow. The left is for primaries between 25 and 50 pc, and the right is for 50–100 pc.

(A color version of this figure is available in the online journal.)

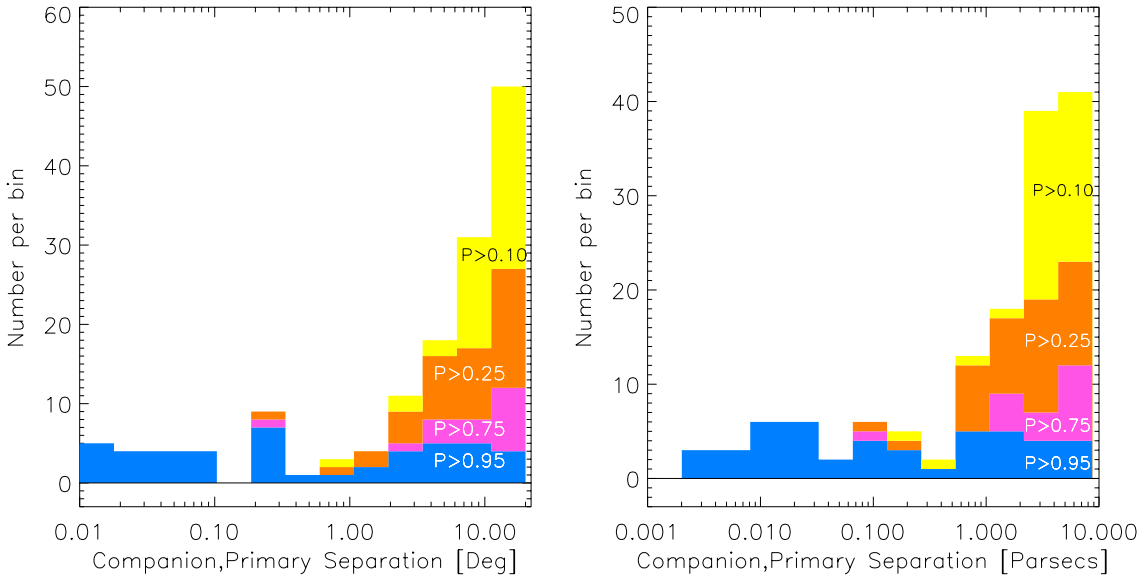

Figure 7. Number and probability vs. separation, 0–25 pc distances—the companion separation histogram for primaries within 25 pc showing the contributions from different probability ranges as in previous figure. The left plot shows angular separation and the right is angular separation times distance to give projected separation in parsecs.

(A color version of this figure is available in the online journal.)

breakdown by probability interval at various separations is presented in Figure 6; the different colored regions show the distribution contoured at 0.1, 0.25, 0.75, and 0.95 probability levels. For the 0–25 pc region, similar information is shown in the left panel of Figure 7. The right panel of Figure 7 presents this information again but with bins of physical projected radius.

4.1. Radial Velocities

Radial velocities differences can be used, where available, as a check on the reasonableness of the probability assignments; therefore we searched the literature for RV measures of HIP stars. Because some RV catalogs in CDS[4] are not incorporated when "querying by identifier" or "querying by coordinate" from SIMBAD, we decided to use SIMBAD plus extract RV catalogs from the CDS archives. A given HIP star may be found in several catalogs and therefore have several values. The data is taken from the six catalogs enumerated below. The order is in increasing reliability and thus increasing priority, e.g., if a later catalog provides a velocity, we use that one. These numbers of obtained radial velocities with distance are plotted in Figure 8 and tabulated in Tables 3–5.

1. *The SIMBAD data base*. While we did extract the RVs in batch mode, the errors could not be obtained in that way. So all RV errors for these stars are set to 10 km s^{-1}. We find 36,884 HIP stars with RV data in SIMBAD.

[4] CDS: Centre de Données astronomiques de Strasbourg; http://cds.u-strasbg.fr/

Table 3
Candidate Companions for 111 Candidate Primaries Within 25 pc

Index	Pri.	Cmp.	ℓ (deg)	b (deg)	V (mag)	Type	μ_l	μ_b	$\Delta\mu_\ell^{\rm cor}$ (mas yr^{-1})	$\Delta\mu_b^{\rm cor}$	d (pc)	v_r	$\Delta v_r^{\rm cor}$ (km s^{-1})	$\mathcal{M}$ ($M_\odot$)	$\Delta\theta d_p$ (pc)	Prob	Comment
(1)	(2)	(3)	(4)	(5)	(6)	(7)	(8)	(9)	(10)	(11)	(12)	(13)	(14)	(15)	(16)	(17)	(18)
1	473		114.6	−16.3	8.20(78)	K6V:;SpB	844.4	−312.7			11.3 ± 0.2	0.6		0.51			
	473	428	114.6	−16.3	9.95	M2e;OtH	826.6	−309.8	21.8 ± 20.3	−4.9 ± 7.7	11.3 ± 0.2	0.3	0.2 ± 0.6	0.45	0.0180	1.000	
2	518		117.0	−3.9	5.98(41)	G5V;SpB	271.7	−17.6			21.5 ± 0.3	−8.0		0.98			
	518	916	117.7	−4.1	9.50	K7;UnK	234.8	−16.9	−26.4 ± 12.1	3.3 ± 3.0	28.1 ± 1.5			0.63	0.2520	0.690	
3	1292		304.9	−37.1	6.59(52)	G8V;YnG	−437.2	−18.3			17.5 ± 0.1	−6.1		0.85			
	1292	107705	319.3	−38.7	9.53	M1Ve;F/E	−432.1	−85.4	−3.5 ± 11.9	−7.8 ± 2.9	16.3 ± 0.4	−4.5	−8.5 ± 10.0	0.50	3.4974	0.620	
4	1349		314.8	−63.7	6.84(57)	G5VFe-;SpB	−243.9	−266.8			22.6 ± 0.3	−11.4		0.80			
	1349	114790	326.4	−55.8	7.96	G7V;OtH	−129.6	−221.2	−3.9 ± 5.8	10.9 ± 6.4	30.7 ± 0.8	−10.7	−7.1 ± 1.7	0.81	3.8576	0.100	
5	1532		97.4	−71.2	9.90 (109)	K5;UnK	−152.3	−267.1			21.1 ± 0.7	−11.1		0.60			
	1532	1539	103.8	−64.7	10.93	−;UnK	−93.1	−199.6	11.7 ± 8.5	18.1 ± 14.4	31.0 ± 2.2			0.54	2.5432	0.190	

(This table is available in its entirety in a machine-readable form in the online journal. A portion is shown here for guidance regarding its form and content.)

Table 4
Candidate Companions for 265 Candidate Primaries between 25 and 50 pc

Index	Pri.	Cmp.	ℓ (deg)	b (deg)	V (mag)	Type	μ_l	μ_b	$\Delta\mu_\ell^{\rm cor}$ (mas yr^{-1})	$\Delta\mu_b^{\rm cor}$	d (pc)	v_r	$\Delta v_r^{\rm cor}$ (km s^{-1})	$\mathcal{M}$ ($M_\odot$)	$\Delta\theta d_p$ (pc)	Prob	Comment
(1)	(2)	(3)	(4)	(5)	(6)	(7)	(8)	(9)	(10)	(11)	(12)	(13)	(14)	(15)	(16)	(17)	(18)
112	493		108.0	−43.3	7.45 (149)	F8;BiN	−181.3	−110.5			37.1 ± 0.8	−45.6		0.94			
	493	495	108.0	−43.5	8.58	K0;BiN	−176.7	−106.3	−4.9 ± 1.9	−4.8 ± 1.9	37.1 ± 1.7	−44.7	−0.8 ± 1.0	0.83	0.1032	1.000	
113	1481		309.1	−53.3	7.46 (150)	F8V;OtH	−100.2	38.1			41.5 ± 0.9	6.6		0.98			
	1481	1910	308.4	−54.7	11.33	M0Ve;BiN	−92.8	39.0	−6.9 ± 7.0	0.8 ± 6.5	53.0 ± 7.6	6.6	−0.1 ± 10.0	0.53	1.0501	0.120	
	1481	1993	308.4	−55.3	11.26	M0Ve;VaR	−96.6	40.9	−3.0 ± 2.5	−0.7 ± 2.7	45.8 ± 5.1	6.4	0.1 ± 10.0	0.57	1.5338	0.930	
	1481	2729	306.3	−55.1	9.56	K4Ve;YnG	−93.1	40.3	−4.6 ± 2.2	2.7 ± 2.1	43.9 ± 1.9	5.7	1.2 ± 10.0	0.75	1.7730	0.900	
114	2484		306.8	−54.0	4.36(22)	B9V;BiN	−90.6	44.9			41.4 ± 0.3	14.0		3.08			β^{01} Tuc; kn: 2487
	2484	1481	309.1	−53.3	7.46	F8V;OtH	−100.2	38.1	6.6 ± 1.6	2.9 ± 1.6	41.5 ± 0.9	6.6	7.1 ± 2.5	0.98	1.1312	0.960	
	2484	1910	308.4	−54.7	11.33	M0Ve;BiN	−92.8	39.0	−0.0 ± 6.9	4.5 ± 6.5	53.0 ± 7.6	6.6	7.0 ± 10.3	0.53	0.8315	0.100	
	2484	1993	308.4	−55.3	11.26	M0Ve;VaR	−96.6	40.9	3.8 ± 2.3	3.5 ± 2.5	45.8 ± 5.1	6.4	7.1 ± 10.3	0.57	1.1710	0.560	
	2484	2578	306.5	−54.0	5.07	A0V;BiN	−92.8	40.4	2.5 ± 1.3	4.8 ± 1.2	45.6 ± 0.4	5.0	9.1 ± 2.8	2.64	0.1108	1.000	β^{03} Tuc
	2484	2729	306.3	−55.1	9.56	K4Ve;YnG	−93.1	40.3	3.1 ± 2.0	6.5 ± 1.9	43.9 ± 1.9	5.7	8.2 ± 10.3	0.75	0.8023	0.940	

(This table is available in its entirety in a machine-readable form in the online journal. A portion is shown here for guidance regarding its form and content.)

Table 5
Candidate Companions for 464 Candidate Primaries between 50 and 100 pc

Index	Pri.	Cmp.	ℓ (deg)	b (deg)	V (mag)	Type	μ_l	μ_b	$\Delta\mu_\ell^{\rm cor}$ (mas yr^{-1})	$\Delta\mu_b^{\rm cor}$	d (pc)	v_r	$\Delta v_r^{\rm cor}$ (km s^{-1})	$\mathcal{M}$ ($M_\odot$)	$\Delta\theta d_p$ (pc)	Prob	Comment
(1)	(2)	(3)	(4)	(5)	(6)	(7)	(8)	(9)	(10)	(11)	(12)	(13)	(14)	(15)	(16)	(17)	(18)
377	185		103.9	−50.3	8.53 (372)	F8;BiN	−78.4	−100.3			77.4 ± 5.5	−7.0		1.11			kn: 190
	185	190	103.9	−50.3	8.74	G0;BiN	−80.3	−97.6	2.0 ± 1.8	−2.7 ± 1.8	87.5 ± 7.1	−6.0	−1.0 ± 6.4	1.00	0.0239	1.000	
378	201		107.1	−42.7	8.24 (320)	F5;OtH	−13.0	23.3			92.2 ± 8.9	−17.6		1.24			
	201	206	107.2	−42.5	8.56	G0;UnK	−11.2	23.7	−1.7 ± 1.6	−0.3 ± 1.5	99.9 ± 9.6			1.25	0.2458	1.000	
379	301		72.1	−75.3	4.55(9)	B9IVn;OtH	−59.2	−33.0			83.5 ± 1.8	8.0		3.01			2 Cet
	301	117821	52.6	−75.8	9.81	F6/F7V;UnK	−63.6	−13.6	−1.1 ± 7.9	1.5 ± 7.4	98.3 ± 23.2			0.95	7.1270	0.210	
380	792		95.1	−67.4	8.43 (350)	G5;UnK	42.1	−40.3			88.0 ± 8.0	24.2		0.97			
	792	976	96.2	−67.9	8.66	F5;UnK	37.3	−41.4	5.1 ± 1.6	2.3 ± 1.7	95.8 ± 8.6			1.22	0.9481	0.420	
381	1266		96.5	−69.9	9.05 (433)	G0;UnK	44.3	−9.2			87.9 ± 9.5			1.02			
	1266	118	86.9	−68.7	9.20	G0;UnK	40.2	−21.9	2.8 ± 2.1	5.6 ± 1.7	77.6 ± 7.3			0.95	5.4860	1.000	

(This table is available in its entirety in a machine-readable form in the online journal. A portion is shown here for guidance regarding its form and content.)

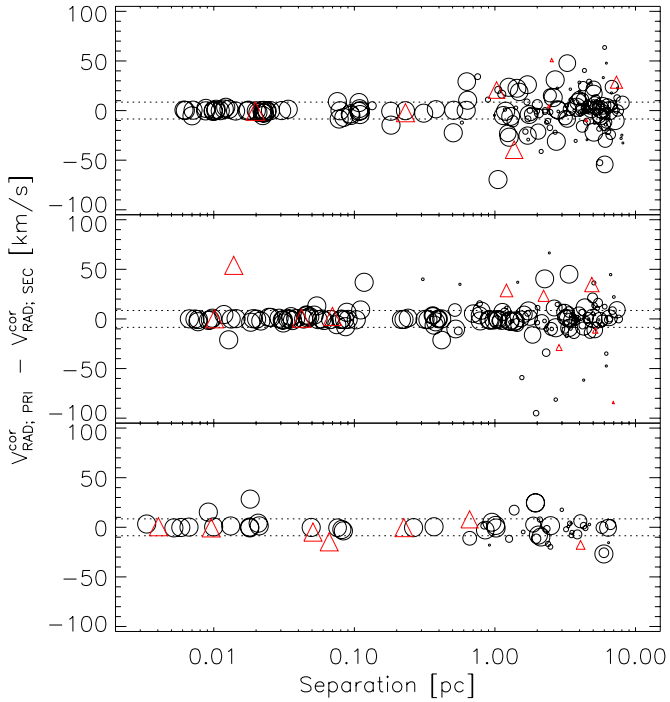

Figure 8. Radial velocity differences—corrected radial velocity differences vs. separation in the plane of the sky in parsecs for *Hipparcos* stars in which radial velocities for both primary and companion are available. Triangles are used for stars listed in the SIMBAD database to be some kind of binary. The size of the symbol is proportional to the probability of companionship down to $P = 0.1$. The primary's space motion is transformed to the direction of the primary to obtain the expected radial velocity of each companion and then the companions' radial velocities are subtracted. The dispersion is much less than expected if randomly drawn from the radial velocities distribution in the solar neighborhood. Since the difference in radial velocity was not used in calculating probabilities, the good agreement of the majority of systems provides high confidence that the technique can find physical companions. The top frame is for primaries between 50 and 100 pc, middle is 25–50 pc, and the bottom is 0–25 pc.

(A color version of this figure is available in the online journal.)

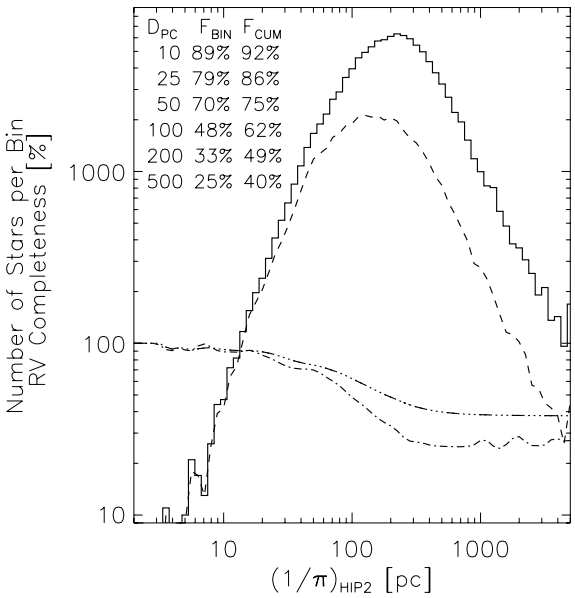

Figure 9. RV statistics of *Hipparcos* stars—the number of HIP stars (per bin) as a function of the inverse of π as listed in HIP2 (histogram; positive parallaxes only). The thick dashed line is the number of stars in our radial velocity database. We show two versions of the completeness of our radial velocity catalog: (1) the completeness per bin (F_{BIN}; thick dash-dotted line) is the ratio of the number of stars with RVs to the number of stars, and (2) the cumulative completeness (F_{cum}; dash-triple-dotted line) which is the total number of stars with RVs up to distance $1/\pi$, divided by the total number of stars out to the same distance. We list both completeness values at some representative distances. Note that, since the typical parallax errors are of order 1–2 mas, distances beyond a few hundred parsec are not very well determined.

2. *The General Catalogue of Mean Radial Velocities* (GCRV; Barbier-Brossat & Figon 2000; VizieR cat. III/213). Following the description in VizieR catalog III/21 (Wilson 1953), the following values for the RV errors based on the quality factors are assigned: quality = A $\rightarrow \epsilon_{RV} = 0.5\ km\ s^{-1}$, q = B $\rightarrow \epsilon_{RV} = 1.2\ km\ s^{-1}$, q = C $\rightarrow \epsilon_{RV} = 2.5\ km\ s^{-1}$, q = D $\rightarrow \epsilon_{RV} = 5.0\ km\ s^{-1}$. Stars with quality E ($\epsilon_{RV} \geqslant 20\ km\ s^{-1}$) are excluded. These errors correspond more or less to the midpoints of the ranges specified by Wilson (1953). We find 21,120 HIP stars in the GCRV.
3. *The Bibliographic Catalogue of Radial Velocities* (BCRV, which is up to date until 2006; Malaroda et al. 2000; VizieR cat. III/249). This catalog required significant attention as it does not list errors on the RVs, while also many stellar names do not conform to the current SIMBAD convention. This may not be too surprising since Malaroda et al. (2000) compiled RV data from almost 1300 different publications. However, the vast majority of stars are found in just 33 different publications. We read those 33 publications and estimated an RV error for each of them. Stars from other publications are, somewhat arbitrarily assigned RV errors of 10 km s^{-1}. There are 1178 stars found in more than one publication, and their weighted average values and errors are used in our database. In total, we find 14,279 HIP stars in the BCRV that are *not* in the GSCN catalog, described below.
4. *The Catalogue of Radial Velocities of Galactic Stars with Astrometric Data, the Second Version* (CRVAD; Kharchenko et al. 2007; VizieR cat. III/254). The same error assignment is used here as for the GCRV above, and stars with RV quality = E are not used. We find 41,740 HIP stars in the CRVAD.
5. *The Geneva-Copenhagen Survey of the Solar Neighborhood* (GCSN; Nordström et al. 2004; VizieR cat. V/117[5]). The "median errors" as listed in the GCSN are used. We find 11,900 HIP stars in the GCSN that were not taken from the GCRV.
6. *The Radial Velocity Experiment: Second Data Release* (RAVE; Zwitter et al. 2008; VizieR cat. III/257). We use the errors as presented in the RAVE catalog. If more than one entry is present per HIP star, the weighted average for both the value and the error are used. We find 393 HIP stars in the RAVE data set.

Altogether, we have 43,047 radial velocities out of 113,942 HIP stars with positive parallaxes: the average completeness is 37.8%. The additional catalogs added 6161 RVs to that available in SIMBAD alone. The completeness fraction is a strong function of distance (Figure 9) and apparent magnitude. About 48% of stars at a distance of 100 pc have a measured RV, but within 100 pc, RV data is available for almost two-thirds of stars. Of the systems where both the primary and candidate have a measured RV, ~87% systems have errors <10 km s^{-1}, with an average of about 1.5 km s^{-1}.

[5] The original catalog V/117 is hard to find on VizieR because it is claimed to be obsoleted by V/130. However, V/130 contains significantly less information, i.e., neither mass estimates nor the raw RV information. This catalog can be accessed by going directly to the source: http://vizier.u-strasbg.fr/viz-bin/VizieR?-source=V/117.

For those stars with RV data in multiple catalogs, we compared the various values to assess their external accuracy. If a star is in fact a binary, then the cataloged values might have been taken at different orbital phases, which would result in a scatter that is larger than expected on the basis of the reported internal errors. We kept track of the range of the reported RVs for a given star, and the errors. If this range exceeds 1.6 times the error *and* the velocity range exceeds 9 km s^{-1}, then the star is deemed to have a discrepant RV, which may be the result of (unsuspected) binarity. About 13% of HIP stars are classified as some sort of binary, while the ones with discrepant radial velocities are classified as binaries about four times more often (∼55%). For our subsample of candidate very wide binaries with discrepant RVs, about 75% are known or suspected binaries. The whole sample of very wide binary candidates has a rate of known/suspected binaries that is 3× larger than for the whole HIP. It is important to note that these known/suspected binaries most often refer to companions closer to our candidates, *not* the candidates we report in this paper. We interpret this as evidence that very wide binaries are often found in hierarchical systems, as suggested by a number of authors (Makarov et al. 2008; Caballero 2009, 2010; Kouwenhoven et al. 2010).

4.2. Stellar Masses

It's useful to obtain mass estimates for the stars in these systems to learn how their separations compare with their nominal tidal radii. Absolute magnitudes (M_V) and stellar masses ($\mathcal{M}$) are assigned based solely on stellar color (B–V), via the mass–luminosity–color relation for the MS. We note that the so-determined $M_V(B–V)$ relation forms a lower envelope to the HIP color–magnitude diagram for MS stars: our relation is close to, but not identical to the zero-age main sequence (ZAMS) $M_V(B–V)$ relation. The starting point is Tables 3.13 and 3.10 in Binney & Merrifield (1998), which list stellar colors, masses and absolute magnitudes as a function of spectral type. Next, the colors are updated in the following way. (1) The *BVRI* colors for O5–M5 stars are taken from Cox (2000), where this source is also used for the values of effective temperature ($T_{\rm eff}$). (2) *BVRI* colors are preferentially taken from Bessell (1990) for types M0–M6. (3) The previous references are superseded by *VRIJHK* data from Bessell (1991) for M6–M7.5 dwarfs. (4) Average $B–V$ colors are computed for late-type M dwarfs by averaging the colors and M_V of several such dwarfs extracted from the NSTARS database.[6] (5) We examine the $B–V$ data for early M dwarfs from Koen et al. (2010), and, to be consistent with the upper MS, we determine a lower-envelope to their HR diagram.[7]

For all cases, we use the dependence of a given color on $T_{\rm eff}$ to interpolate over missing values.[8] Then, for each star, their $B–V$ values are used to compute their MS masses. However, still not all stars have $B–V$ values, and we estimate their masses from the weighted average of a number of other color–mass relations: $\mathcal{M}_{V-I}$, $\mathcal{M}_{V-J}$, $\mathcal{M}_{V-H}$, $\mathcal{M}_{V-K}$, $\mathcal{M}_{J-H}$, $\mathcal{M}_{J-K}$, $\mathcal{M}_{H-K}$, and $\mathcal{M}_{H-K}$.[9]

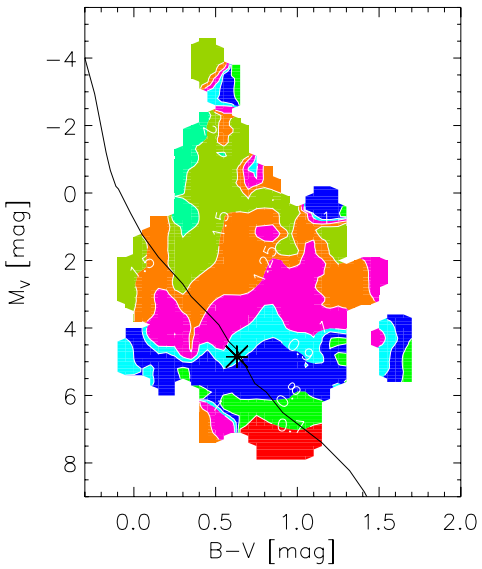

Figure 10. GCSN mass map—the mass as determined from the GCSN as a function of (B–V) color (abscissa) and absolute magnitude (ordinate). The contours are labeled by the mass values The solid line represents the main sequence, and the star-symbol the location of the Sun. The fact that the Sun does not lie in the $\mathcal{M} = 1$ contour, but at $\mathcal{M} = 0.925$, indicates that the errors on the inferred masses are not negligible: about 7.5% on the MS, about 15% below the MS and up to 20% towards the top and right-hand side of the map.

(A color version of this figure is available in the online journal.)

Lastly, a correction is made for the effects of stellar evolution as stars evolve off the ZAMS. The GCSN catalog (Nordström et al. 2004) provides stellar masses corrected for stellar evolutionary effects, absolute magnitudes and (B–V) colors for 14,955 HIP stars. We compute a two-dimensional look-up table (map), with the average mass as a function of (B–V) and M_V. This contour map, Figure 10, shows for any star that falls in a defined part of the map, the corresponding mass value used. For stars in undefined parts of the map, the color–mass relation for the MS is used. The masses are listed in Column 14 of Tables 3–5. Note that these masses are insufficient to decide whether or not a potential pair is bound because, quite often, the system contains stars that are not a part of HIP.

4.3. Tabulated Results

The focus of this research has been on very wide companions in the 25–100 pc interval; however, we have applied a similar methodology to the 0–25 pc interval even though it has not been optimized for this regime. Fortunately, a number of high probability companions are discovered in this region out to 20° in separation. The physical systems and their probabilities are presented in Tables 3–5 for the distance ranges 0–25 pc, 25–50 pc and 50–100 pc, respectively. The names (Columns 1 and 2), positions (Columns 3 and 4) and the visual magnitude (Column 5) are taken from HIP. The spectral type (Column 6) is taken from SIMBAD.[10] We also list in this column one of 10 possible types on the basis of the 67 "Other object type" identifications in SIMBAD (such as, "*in**," "EB," "YSO," mean: "star in double star," "Eclipsing binary" and "young stellar object," respectively). The codes are: UkN (not known),

[6] We estimate $B–V = 1.91 \pm 0.064$, 1.99 ± 0.009, 2.05 ± 0.078, 2.16 ± 0.8 and 2.10 for types M5.5, M6.0, M6.5, M7.0 and M8.0, respectively.

[7] We use: $B–V = 1.47$, 1.51, 1.577, 1.677 for types M1, M2, M3 and M4, respectively.

[8] Not all stars in HIP have $B–V$ colors. Furthermore, because the $B–V$ colors in HIP are derived in a non-homogeneous manner (partly derived from ground-based observations and partly from the TY1 photometry), we use our own estimation for the $B–V$ values on the Johnson system based on TY2 colors: $(B–V)_J = 0.85\,(B–V)_{T2}$. This transformation is accurate to ± 0.071 mag, which is 2.2 times larger than the errors on $B–V$ as listed in HIP. Note that we use the TY2 colors, which differ substantially (at fainter magnitudes) from the TY1 colors listed in HIP.

[9] The J, H, and K magnitudes (and errors) are extracted from the 2MASS database.

[10] http://simbad.u-strasbg.fr/simbad/

SpB (spectroscopic binary), EcB (eclipsing binary), BiN (other binary), RoT (star with high rotation velocity), VaR (variable star), YnG (young/pre-MS star), ClN (star in cluster of nebula), F/E (flare or eruptive star), OtH (generic star or other object).

The proper motions (Columns 7 and 8) are from TY2 when available, otherwise they are from HIP2. Columns 9 and 10 list the proper-motions differences *corrected* for geometric effects as described in Section 3.2 above. In detail, our procedure is as follows. First, for each potential primary star, its space velocity (v_x, v_y, v_z) is computed according to Equations (31)–(33) using its distance, proper motions, and radial velocity, if available. In the next step, this space velocity is transformed into the expected proper motions if it were at the positions of the companions. However, beyond 25 pc, the distance to the primary is used as the distance to its companion because $P(\Delta\mu \mid c)$ is meant to give the probability of having $\Delta\mu$ assuming that it is a companion, and should not be reduced by a large distance error. Beyond ~25 pc, the typical parallax errors, imply distance errors that significantly exceed the orbit size and would artificially inflate the inferred proper-motion corrections. We use the RV of the primary because it is usually the better studied and, therefore, is more likely to provide the barycentric velocity of the system.

The corrected proper-motion differences listed in Columns 9 and 10 are the difference between the proper-motion components of the primary and the candidate if it were seen with the same projections onto the sky as the primary. In the same columns, the errors on these $\Delta\mu^{\rm cor}$ values are listed, which are derived via propagating the errors on the observables. The procedure inflates the observed proper-motion errors, typically by factors of 2 to 4. This is to be expected because the corrected proper-motion difference contains three or four terms (cf. Equation (29)) that are combined in quadrature to yield the errors. The distance (Column 11) is the inverse of π obtained from HIP2. Column 12 contains the radial velocities compiled in Section 4.1. For Column 13, the proper motion and RV of the companion are transformed to LSR space velocities at its position and then the RV is calculated from that space velocity translated to the position of the primary. Beyond 25 pc, we again use the primary's distance in the first step instead of the companion's to minimize correction errors due to distance uncertainties. The errors on the corrected RVs are nearly the same as the errors on the measurements themselves because the corrections are typically small. The RV differences are plotted in Figure 8. The separation (Column 15) follows from the positions of the primaries and companions and the distance of the primary.

Column 16 gives the probability of the candidate being a true companion of the primary according to Equation (5).

The last column (17) provides Bayer–Flamsteed (BF) designations and common names for the stars. These are extracted from the "HD-DM-GC-HR-HIP-Bayer–Flamsteed Cross Index" (Kostjuk 2004), with the following modifications: (1) a common name is not listed if the same name is used for another HD star, unless the system is a close pair, (2) if more than one common name was specified, the shortest one is used. Note that in some cases, Kostjuk (2004) uses as the BF designation *both* the numeric and the Greek designation. If the star has another HIP star as a companion (as listed in HIP), we add the known HIP numbers after the "kn": designation.

4.4. Some Notable Companion Pairs

We find these unnoticed naked-eye companions (<6th mag): Capella & 50 Per, δ Vel & HIP 43797, Alioth (ϵ UMa),Megrez (δ UMa) & Alcor, γ & τ Cen, ϕ Eri & η Hor, 62 & 63 Cnc, γ & τ Per, ζ & δ Hya, β^{01}, β^{02} & β^{03} Tuc, N Vel & HIP 47479, HIP 98174 & HIP 97646, and s Eri & HIP 14913. High probabality fainter companions (>6th mag) of stars $V < 4$ are found for: Fomalhaut (α PsA), γ UMa, α Lib, Alvahet (ι Cephi), δ Ara, Chow (β Ser), ι Peg, β Pic, κ Phe, and γ Tuc.

4.4.1. The Capella System

We identify the T Tauri star 50 Per (HIP 19335) as a $P = 0.2$ candidate companion of Capella. While these stars have almost equal radial velocities and corrected proper-motion differences, they are separated by almost 15° on the sky (5.4 pc) and have a three-dimensional separation of 8.9 pc. The corrected proper-motion differences (~12 ± 5 mas yr^{-1}) may seem a bit too large to accept this system as a real wide-binary candidate, but this difference is time dependent. Capella is an almost equal-mass spectroscopic binary with component masses 2.466 and 2.443 $M_\odot$. It has, 12′ away, known companion WDS 05167+4600 HL which comprises the M1V star GJ 195 A ($V = 10.16$ mag) and the M5 dwarf GJ 195 B ($V = 13.7$ mag), which are separated by 6″. 50 Per itself is paired here with HIP 19255 at a separation of ~15,200 AU (~740″). Furthermore, the MSC identifies both 50 Per and HIP 19255 as possible binaries themselves, while these systems orbit each other in about one million years at an equivalent circular orbit speed of ~0.45 km s^{-1} (4.8 mas yr^{-1}). The MSC reports a total mass 3.64 $M_\odot$ for the 50 Per and HIP 19255 system. The two components of HIP 19255 are separated by 3.″87 and orbit each other in 590 years ($v_{\rm orb}$ ~ 4 km s^{-1} = 42.5 mas yr^{-1}). This orbital speed is more than sufficient to account for the corrected proper-motion difference between 50 Per and HIP 19255. We find the following about the putative 50 Per binary: (1) The HIP2 and TY2 proper motions for 50 Per differ by 2.7 ± 1.7 mas yr^{-1}, (2) HIP finds an acceleration in the proper motion which Makarov & Kaplan (2005) estimate to be 5.8 ± 3 mas yr^{-2} (~0.5 km s^{-1} yr^{-2}), and (3) the GCSN reports 8 observations over a period of seven years with measurements errors of 0.2 km s^{-1} and an ensemble error of 0.6 km s^{-1}: this is consistent with an acceleration of 0.286 ± 0.06 km s^{-1} yr^{-2}. Thus, both RV and proper-motion data indicate the presence of an unseen companion for 50 Per. The corrected proper motion and RV differences between 50 Per and Capella are bridged at the observed accelerations of 50 Per after 4 ± 3 and 17 ± 4 yr, respectively.

The total mass for the Capella/50 Per system is (5.88+3.64) = 9.52 $M_\odot$, so that the Jacobi radius is 2.8 pc, or about three times smaller than the observed separation. Thus, Capella and 50 Per may be an example of an escaped binary system.

Although we also list the known double, HIP 26779 and HIP 26801, at 509′ or 2 pc from Capella as having very high probability for being physically related to Capella, unless the RV is just wrong, we suspect that these are false positives. The barycentric velocity is well established, therefore the ~ 25 km s^{-1} difference in radial velocities is hard to explain unless this system is just passing by.

5. CONCLUSIONS

We have applied a full Bayesian approach to assigning probabilities of companionship between HIP stars separated by more than 0.01 pc. By companionship we mean either bound gravitationally as in a system of small numbers of stars or co-moving with nearly the same velocity as in an escaped

previously bound component. After subtracting the expected numbers of false positives derived from control experiments, a population of companions extending out to 8 pc in separation remains. Some of these very wide systems contain hierarchies of fairly massive stars that extend the tidal radii out to unusually large distances, but it is likely that others are recently unbound systems that continue to travel along nearly the same trajectory. While some of these seem to be parts of known nearby moving clusters or associations (e.g., Tucanae Stream, Hyades Stream, UMa Moving Cluster, β Pic Moving Group, and TW Hydrae Association), this procedure brings to focus even higher density knots within them, which should be far more persistent than the rest of the association either as a bound system or a tight stream. The amount of time after breakup of an open cluster or binary system for which companions stay in close proximity may be an important constraint on the mass and distribution of dark matter candidates such as dark subhalos.

Our statistical method finds both many highly significant pairings that are missed by previous techniques and assigns reasonable probabilities for companions even in regions previously considered too complicated or crowded. In the 1–100 pc distance range, we find altogether ∼222 high probability HIP–HIP companions with separations between 0.01 and 1 pc, and we find strong evidence for a population of companions separated by 1–8 pc with ∼314 stars. In just the 0–25 pc range, we find ∼34 companions with separations 0.01–1 pc and ∼50 companions with separations 1–8 pc. Our preliminary investigations do not show any obvious trend for the excess of wide/escaped binaries along the Galactic rotation direction.

As displayed in Figure 8, we find good agreement between the radial velocities of the primary and the corrected RV of the candidate companions: 56% have velocity differences $<6.8\ \mathrm{km\,s^{-1}}$ (about 3σ). For comparison, the distribution of RV differences of random nearby HIP–HIP pairs closely resembles a zero-centered Gaussian with a dispersion of $\sim 37.5\ \mathrm{km\,s^{-1}}$, which leads to a 15.8% chance that a random pair would have a velocity difference as small as $6.8\ \mathrm{km\,s^{-1}}$. In addition, unresolved spectroscopic binaries can induce RV differences of order $10–30\ \mathrm{km\,s^{-1}}$, and so pairs with substantial RV differences might in fact be physically associated. Therefore, the fraction of pairs with small true RV differences could be significantly higher.

In some individual cases, such as Capella two of its candidate companions (HIP 26779 & 26801), the RV data indicates that the candidates are not real. Out of 426 candidates with radial velocities, we find 187 (44%) pairs for which the corrected radial velocities deviate by more than three times the errors: most of these systems might qualify as false positives. This rate of potential false positives agrees excellently with the rate identified in the control experiments (Figure 5 and Table 5) of 428 control candidates out of 964 HIP candidates or 44%.

Figures 2 and 4 indicate that the classical log-normal period distribution (DM91) results in a distribution of pair separations that is very different from the one we observe. To double check this, we use another simulation, where *each* HIP star is assigned a secondary with a mass drawn from the initial mass function. The absolute magnitudes for these simulated stars are estimated by applying the inverse of the procedure outlined in Section 4.2 above. We then use the magnitude–completeness function of HIP (as determined by comparing it to the TY2 magnitude counts) to decide to accept or reject a given simulated secondary. While this procedure more-or-less reproduces the *number* of known HIP–HIP binaries, the distribution of separations resembles the results obtained from our simulation (Figure 2), but at lower amplitude. An attempt was made to match more closely our observed distribution by changing the location and width of the peak of the log-normal period distribution, and the form of the IMF. None of these experiments succeeded. We tentatively conclude that the observed distribution of separations is incompatible with the log-normal period distribution of nearby G-type field stars as observed by Duquennoy & Mayor (1991). However, we also must acknowledge that the non-random selection of fainter stars in HIP and the fact that this catalog is magnitude limited renders extractions of overall statistics on true binarity rates quite uncertain.

The very wide systems found here are all smaller than $6.2\ r_J$ and seem to be distributed as suggested by Jiang & Tremaine (2010), with a minimum at about r_J, and a rising population of escaped companions at larger separations. The relative velocities are a more stringent criterion: from Figure 6 of Jiang & Tremaine (2010), we infer that escaped binaries should have $\Delta v/v_J \lesssim 30$. About 72% of the our systems satisfy this criterion. Including the observational errors, 89% (98%) of our very wide systems satisfy the criterion within 1σ (2σ). Thus, we are confident that most of these systems qualify as bona fide escaped bound systems.

However, they may not have begun as simple binary sytems. Other possible sources are the remnants of dissolving low-density clusters of stars. Kouwenhoven et al. (2010) show that dissolving clusters can produce very wide binaries whose separation can easily reach parsecs, and even have rising distributions at separations around one parsec. In fact, Kouwenhoven et al. (2010) argue that the size of the semi-major axis of *young* wide binaries is similar to the initial size of the cluster from which they formed. Our systems are moderately young (typical mass $1.5\ M_\odot$), and so the bound ones may still reflect the size of their birth places. Another prediction Kouwenhoven et al. (2010) make is that very wide binaries should be preferentially hierarchical with each of the wide components being binaries by themselves. Indeed there are observations that are consistent with this prediction (Makarov et al. 2008; Caballero 2009, 2010). For the few systems that we have thus far tried to collect possible companions from the literature, we do indeed find a preponderance of hierarchical systems.

We have discovered some hitherto unnoticed pairing of very nearby stars and a large number of pairings at record separations. Subhalos would greatly accelerate the disruption of wide binaries if they are an important contributor to the small scale potential locally in the Galaxy. Unfortunately, the distribution of subhalos in the Galaxy at the solar radius is not yet well predicted by *N*-body or hydrodynamical simulations (Gan et al. 2010). Since companionship of escaped binary companions at large separations is very fragile, requiring comoving velocities to remain $\lesssim 1\ \mathrm{km\,s^{-1}}$, statistics on the number of very wide companions and their ages should lead to useful limits on the masses and number densities of dark matter subhalos.

Statistical algorithms for ascertaining probabilities of association and/or boundedness in large astrometric surveys with high precision will become more effective as larger and more precise astrometric surveys come along, such as Pan–Starrs (Chambers 2005), LSST (Ivezić et al. 2008), and *Gaia* (Perryman 2002; Lindegren et al. 2008). The astrometric data from Gaia will be about 10 times better than the positional data obtained from the former two ground-based projects. When available, such data will enable a full mapping of the six-dimensional phase-space

distribution of any potential physical binary. To facilitate the analysis of these future catalogs, as well as the analysis of the existing astrometric catalogs, we investigated the reliability of Bayesian algorithms for providing realistic probabilities of extremely wide companions and found it to be quite successful even when implemented in only simplified form. In the future, we hope to make more complete statistical use of measurement errors, magnitude binning, and incorporation of radial velocities and to apply these to the full TY2.

We thank Scott Tremaine for some useful discussions. E.J.S. and R.P.O. were partially supported by the SIM project which is carried out for NASA by JPL under a contract with the California Institute of Technology. In this work, we made extensive use of the *Hipparcos* and Tycho-2 Catalogues (ESA 1997; van Leeuwen 2007). This work would have been virtually impossible without the aid of the SIMBAD database, operated at the "Centre de Données astronomiques de Strasbourg" (CDS). R.P.O. was supported by an inheritance from his late father, Dr. Ch. C. J. Olling.

REFERENCES

Bahcall, J. N., & Soneira, R. M. 1981, ApJ, 246, 122
Barbier-Brossat, M., & Figon, P. 2000, A&AS, 142, 217
Bessell, M. S. 1990, A&AS, 83, 357
Bessell, M. S. 1991, AJ, 101, 662
Binney, J., & Merrifield, M. 1998, Galactic Astronomy (Princeton Series in Astrophysics; Princeton, NJ: Princeton Univ. Press)
Caballero, J. A. 2009, A&A, 507, 251
Caballero, J. A. 2010, A&A, 514, A98
Chambers, K. C. 2005, in ASP Conf. Ser. 338, Astrometry in the Age of the Next Generation of Large Telescopes, ed. P. K. Seidelmann & A. K. B. Monet (San Francisco, CA: ASP), 134
Chanamé, J., & Gould, A. 2004, ApJ, 601, 289
Cox, A. N. 2000, Allen's Astrophysical Quantities (4th ed.; Melville, NY: AIP), 388
Duquennoy, A., & Mayor, M. 1991, A&A, 248, 485 (DM1991)
Eggleton, P. P., & Tokovinin, A. A. 2008, MNRAS, 389, 869
ESA 1997, The Hipparcos (HIP) and Tycho Catalogs (TY) (Noordwijk: ESA Publ. Division, ESTEC)
Fabricius, C., Høg, E., Makarov, V. V., Mason, B. D., Wycoff, G. L., & Urban, S. E. 2002, A&A, 384, 180
Gan, J., Kang, X., Van Den Bosch, F., & Hou, J. 2010, MNRAS, 408, 2201
Goldberg, D., Mazeh, T., & Latham, D. W. 2003, ApJ, 591, 397
Goodwin, S. P. 2010, Phil. Trans. R. Soc. A, 368, 851
Goodwin, S. P., Kroupa, P., Goodman, A., & Burkert, A. 2007, in Protostars and Planets V, ed. B. Reipurth, D. Jewitt, & K. Keil (Tucson, AZ: Univ. Arizona Press), 133
Gould, A., & Chanamé, J. 2004, ApJS, 150, 455
Gould, A., & Kollmeier, J. A. 2004, ApJS, 152, 103
Heggie, D. C. 1975, MNRAS, 173, 729
Høg, E., et al. 2000, A&A, 357, 367 (TY2)
Hogeveen, S. J. 1990, Ap&SS, 173, 315
Ivezić, Ž., et al. 2008, in IAU Symp. 248, A Giant Step: from Milli- to Micro-arcsecond Astrometry (Cambridge: Cambridge Univ. Press), 537
Jiang, Y.-F., & Tremaine, S. 2010, MNRAS, 401, 977
Kharchenko, N. V., Scholz, R.-D., Piskunov, A. E., Röser, S., & Schilbach, E. 2007, Astron. Nachr., 328, 889
Koen, C., Kilkenny, D., van Wyk, F., & Marang, F. 2010, MNRAS, 403, 1949
Kostjuk, N. D. 2004, VizieR Online Data Catalog, IV/27
Kouwenhoven, M. B. N. 2006, PhD thesis, Univ. of Amsterdam
Kouwenhoven, M. B. N., Brown, A. G. A., Goodwin, S. P., Portegies Zwart, S. F., & Kaper, L. 2009, A&A, 493, 979
Kouwenhoven, M. B. N., Goodwin, S. P., Parker, R. J., Davies, M. B., Malmberg, D., & Kroupa, P. 2010, MNRAS, 404, 1835
Kuiper, G. P. 1942, ApJ, 95, 201
Lépine, S., & Bongiorno, B. 2007, AJ, 133, 889
Lépine, S., & Shara, M. M. 2005, AJ, 129, 1483
Levine, S. E. 2005, AJ, 130, 319
Lindegren, L., et al. 2008, in IAU Symp. 248, A Giant Step: from Milli- to Micro-arcsecond Astrometry (Cambridge: Cambridge Univ. Press), 217
Malaroda, S., Levato, H., Morrell, N., García, B., Grosso, M., & Bolzicco, G. J. 2000, A&AS, 144, 1
Makarov, V. V., & Kaplan, G. H. 2005, AJ, 129, 2420
Makarov, V. V., Zacharias, N., & Hennessy, G. S. 2008, ApJ, 687, 566
Mason, B. D., Wycoff, G. L., Hartkopf, W. I., Douglass, G. G., & Worley, C. E. 2001, AJ, 122, 3466
Monet, D. G., et al. 2003, AJ, 125, 984
Nordström, B., et al. 2004, A&A, 418, 989 (VizieR Online Catalog, V/117)
Olling, R. P. 2005, in ASP Conf. Ser. 338, Astrometry in the Age of the Next Generation of Large Telescopes, ed. P. K. Seidelmann & A. K. B. Monet (San Francisco, CA: ASP), 272
Öpik, E. 1924, Tartu Obs. Publ., 25, 6
Parker, R. J., Goodwin, S. P., Kroupa, P., & Kouwenhoven, M. B. N. 2009, MNRAS, 397, 1577
Perryman, M. A. C. 2002, Ap&SS, 280, 1
Pourbaix, D., et al. 2004, A&A, 424, 727
Quinn, D. P., Wilkinson, M. I., Irwin, M. J., Marshall, J., Koch, A., & Belokurov, V. 2009, MNRAS, 396, L11
Raghavan, D. 2009, PhD thesis, Georgia State Univ. (http://www.chara.gsu.edu/~raghavan/thesis/dissertation.pdf)
Retterer, J. M., & King, I. R. 1982, ApJ, 254, 214
Skrutski, M. F., et al. 2006, AJ, 131, 1163
Unwin, S. C., et al. 2008, PASP, 120, 38
van Leeuwen, F. 2007, [HIP2], A&A, 474, 653
Weinberg, M. D., Shapiro, S. L., & Wasserman, I. 1987, ApJ, 312, 36
Wilson, R. E. 1953, General Catalogue of Stellar Radial Velocities (VizieR On-line Data Catalog, III/21; Washington, DC: Carnegie Inst.)
Zacharias, N., Urban, S. E., Zacharias, M. I., Wycoff, G. L., Hall, D. M., Monet, D. G., & Rafferty, T. J. 2004, AJ, 127, 3043
Zacharias, N., et al. 2010, AJ, 139, 2184
Zwitter, T., et al. 2008, AJ, 136, 421